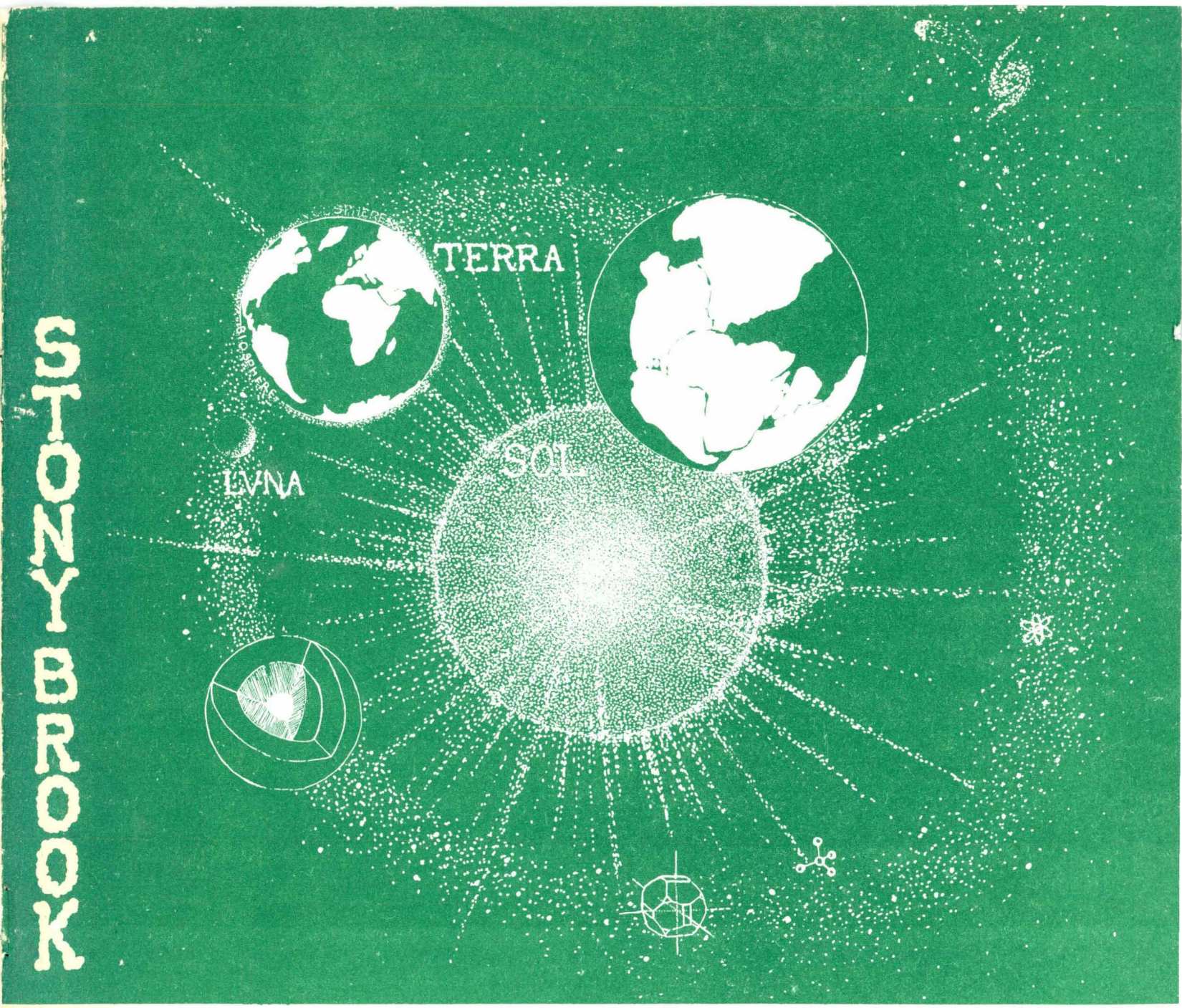

Chemistry and Petrology of Size Fractions of Apollo 17 Deep Drill Core 70009-70006.

J. C. Laul
Earth and Planetary Chemistry Section
Physical Sciences Department, Battelle-Northwest
Richland, Washington 99352

D. T. Vaniman, J. J. Papike and S. Simon
Planetary Regolith Studies
Department of Earth and Space Sciences
State University of New York
Stony Brook, New York 11794

In Press: 9th Lunar and Planetary Conference Proceedings
June 1978

ABSTRACT

We have used INAA methods to analyze 34 major, minor and trace elements in 48 bulk soils and size fractions (90-1000 μm, 20-90 μm and <20 μm) of the Apollo 17 deep drill core sections 70009-70006 (upper 130 cm). Modal data were also obtained for the >20 μm size fraction. The cores are highly heterogenous chemically and petrographically. The >90 μm and 20-90 μm coarse fractions are chemically identical but different from the <20 μm fine fraction. The coarse fractions are highly enriched in mare material (high Ti basalt + orange glass) in sections 70009 and 70008; the 28, 38 and 47 cm layers of coarse core 70008 are almost entirely mare material. Below 58 cm depth, mare material decreases and highland material increases with increasing depth. The <20 μm fine fraction comprises about 15-25 wt. % of the bulk soil and is considerably enriched in highland material. Except for the coarse section 70008, highland material in the <20 μm fraction increases with increasing depth. The dominant source of highland material is KREEPy and mafic instead of anorthositic. Relative to the coarse fractions, the fine fractions contain ∿10% more low-K KREEPy material. Low-K KREEP can be obtained by lateral transport of fines from the local massifs (Korotev, 1976). Enrichment of KREEP in the Apollo 17 fines follows similar observations at other sites (Apollo 11 soil 10084 and Apollo 15 soil 15100) and points to enhanced transport of fines on a moonwide basis, with the constraint that local sources predominate at each site.

INTRODUCTION

The regolith at the Apollo 17 site is quite complex due to the interface of mare and highland materials at the Taurus-Littrow site. In order to characterize and understand the formation of the regolith, we have focused our attention on the Apollo 17 deep drill core. The Apollo 17 drill core (sections 70009-70001) represents the deepest soil column (295 cm) returned from the moon. This core was collected at the ALSEP site, about one crater diameter SE of the 400 m Camelot crater and NW of the "Central Cluster" craters, and is believed to contain ejecta from these craters (LSPET, 1973, Duke and Nagle, 1974; Taylor et al., 1977). The neutron fluence study of Curtis and Wasserburg (1975) suggests that the entire drill core was deposited less than 200 m.y. ago, a conclusion which places an upper age limit on nearby contributing craters. From track studies in 70009 and 70008 Crozaz and Plachy (1976) suggest that the upper 80 cm were emplaced some 100 m.y. ago, and the upper 25cm was recently ($\sim$2 m.y.) excavated by a small impact and was then gradually filled by heavily irradiated surface soil.

The entire core has three major stratigraphic units: an upper, coarse-grained interval (107 cm) dominated by mare basalt fragments; a middle, fine-grained interval (56 cm) consisting mainly of highland material; and a lower interval (132 cm) containing a variety of breccias and crystalline fragments (LSPET, 1973). These major stratigraphic units can be subdivided on the basis of X-radiography or core dissection observations (Duke and Nagle, 1974). Ehmann and Ali (1977) analyzed 26 bulk samples from 70009-70007 for major and trace elements by INAA, and they reported 10 chemical units that were distinct

from the 12 X-ray units and 19 stratigraphic units of Duke and Nagle (1974). Based on petrographic observations, Vaniman and Papike (1977a,b) and Taylor et al., (1977) suggested three major zones in 70009-70007. an upper zone (0 to 21 cm) characterized by high agglutinate content; a middle zone (22 to 66 cm) characterized by low agglutinate content and high abundance of coarse mare basalt fragments, and a lower zone (67 to 100cm) distinguished by medium agglutinate content and a large quantity of non-mare lithic fragments. These three zones are consistent with breaks in the FMR maturity index (Morris et al., 1978): Section 70009 is submature, 70008 is immature, and 70007 is submature. Vaniman and Papike (1977a) characterized >20 μm lithic and mineral fragments in 70009-70007 and suggested that the anorthositic component predominates over the noritic (KREEPy) component in the upper drill core (70009, 70008), but noritic compositions become more abundant in 70007 where the mare component decreases and the highlands component increases.

Korotev (1976) analyzed major and trace elements in size fractions of 90-150 μm and <20 μm from 70008 and seven surface soils and noted that the 90-150 μm fraction is enriched in mare material (basalt plus orange glass), whereas the <20 μm fraction is feldspathic in composition and enriched in highland material and some orange glass. Korotev (1976) investigated in detail the processes responsible for the observed chemical differences in the two size fractions, and showed that the differences can be explained by mixing distinct components. Chemical differences can also result between different size fractions of comminuted lunar basalt (Haskin and Korotev, 1977). However, Korotev (1976) showed that the later process is a second-order effect in the compositional differences between size fractions of the Apollo 17 soils. He used

DEPTH, cm	PARENT #	SAMPLE #
0.6 - 1.1	9	432
9.1 - 9.6	45	433
20.1 - 20.6	99	434
27.8 - 28.3	153	455
37.7 - 38.2	110	456
46.8 - 47.3	72	457
57.3 - 57.8	30	458
70.4 - 70.9	120	167
80.9 - 81.4	58	168
89.4 - 89.9	24	169
97.7 - 98.2	36	16
108.2 - 108.7	79	17
117.2 - 117.7	116	18
130.2 - 130.7	167	19

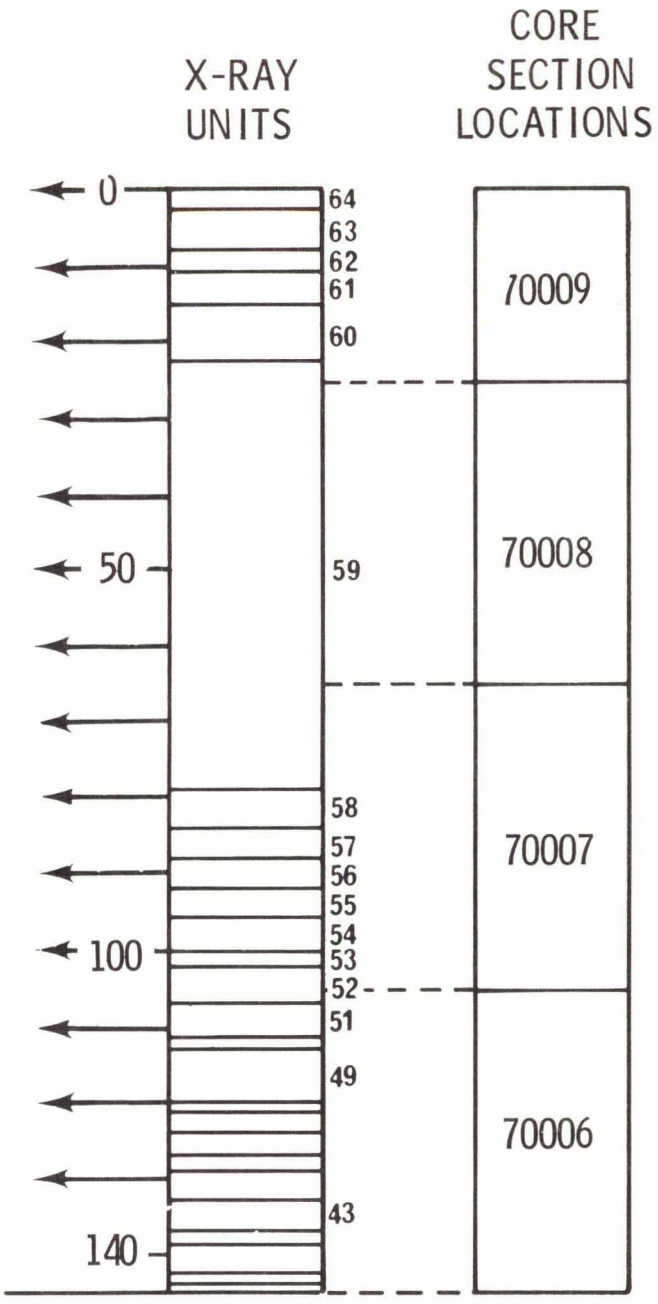

Figure 1. X-ray stratigraphy and core section locations, 70009-70006. Locations are shown for sample numbers used for chemical-petrographic studies.

a multielement mixing model with 5 components and reported ∿30% highland material in 1:1 proportions of noritic breccia (KREEP) and anorthositic gabbro in <20 μm fraction of 70008. We studied three size fractions (90-1000 μm, 20-90 μm and <20 μm) from core sections 70009-70006 and our findings in <20 μm fraction of 70008, using Th as an indicator for KREEP, are consistent with Korotev's observations. We point out that the present work on 70009-70006 is part of our ongoing study of the 70009-70001 core sections. Thus, detailed quantitative treatment of the data by a multielement mixing model will await the completion of our studies of core sections 70005-70001. In this paper we focus on general features and characterization of the <20 μm fractions. Since the <20 μm soil fraction is different from the coarser soils, its chemistry is exceedingly important in understanding lateral and vertical regolith mixing. In addition, the chemical information from the >20 μm fraction is important to test the approach of chemical mixing by modal recombination techniques as demonstrated for drive tube 60009/60010 core by Papike et al., 1978 and Vaniman et al., 1978. Although some preliminary conclusions are discussed below, the primary purpose of this paper is to present detailed chemical data for use by the research community prior to completion of our long-term study.

In our chemical-petrographic consortium effort, we selected 14 soils (<1 mm size fraction) from about 10 cm depth intervals in core sections 70009-70006. The sample number, parent number, and corresponding depth intervals are shown in Figure 1. Each soil was sieved into three size fractions (90-1000 μm, 20-90 μm and <20 μm). These soil fractions were studied by instrumental neutron activation (INAA) at Battelle-Northwest (BNW), whereas petrologic studies of >90 μm and 20-90 μm fractions were

done at Stony Brook. A complete string of polished thin sections that represent the full length of core sections 70009-70006 has been examined by the Stony Brook group. The detailed mineralogy, petrology and stratigraphy of sections 70009-70007 are already published (Vaniman and Papike, 1977a,b). The modal data for new grain mounts from depths corresponding to the BNW chemical study on sections 70009-70006 are discussed here.

METHODS

SIEVING

About 80 mg of each bulk soil (<1 mm fraction) were sieved into three size fractions (90-1000 μm, 20-90 μm and <20 μm) in the clean facility of Dr. D. S. McKay at JSC using the procedure of McKay et al. (1974). Intermediate sieve sizes of 45 μm and 150 μm were used to facilitate sieving operations. Ultrapure Freon TF (DuPont) was used throughout the sieving operations. The material loss in sieving operations was typically 10%, largely from the <20 μm fraction. A small aliquot from each 90-1000 μm and 20-90 μm size fraction was reserved for petrographic study at Stony Brook, while the remaining material (along with the <20 μm fraction) was used for INAA analysis at Battelle-Northwest. To check the mass-balance of sieved fractions, several small aliquots of bulk soil were saved prior to sieving.

Figure 2 displays the percentage weight recoveries in 90 μm, 20-90 μm and <20 μm size fractions of each soil. The weight of the

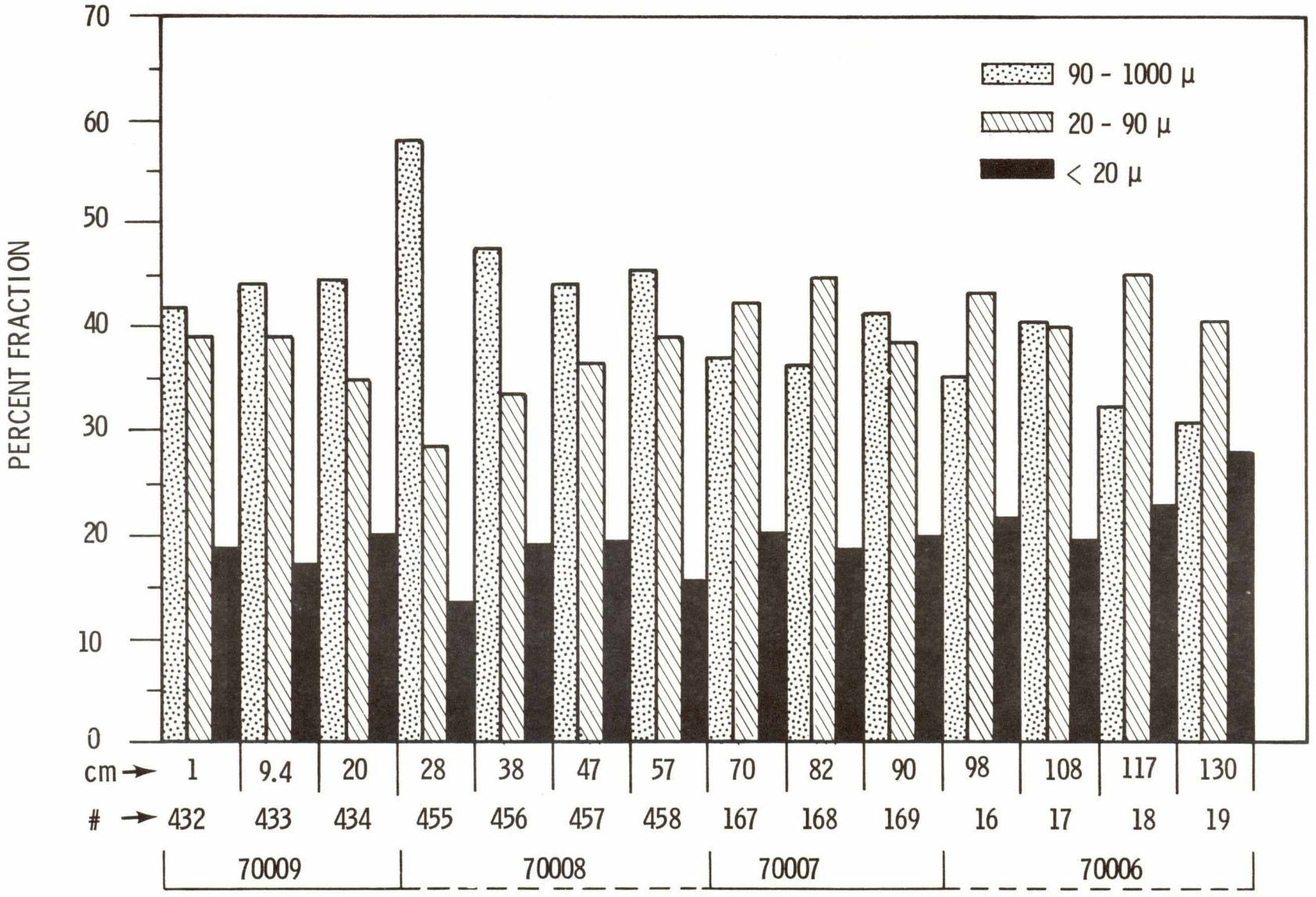

Figure 2. Percent weight recoveries in 90-1000 µm, 20-90 µm and <20 µm size fractions of soils in 70009-70006.

<20 μm size fraction varied from 15-25% and was generally ∿20% of the bulk soil weight. The >90 μm and 20-90 μm fractions were about equal in weight proportion in core sections 70009, 70007 and 70006, but the >90 μm fraction was significantly greater in 70008 reflecting the dominance of a coarse grained layer.

INSTRUMENTAL NUETRON ACTIVATION ANALYSIS (INAA)

Soils were analyzed by sequential INAA using a high efficiency 130 cc Ge(Li) detector (25%, FWHM 1.8 KeV for 1332 Kev γ of ^{60}Co), a 2048 channel analyzer, and employing the unique BNW coincidence and non-coincidence Ge(Li)-NaI(Ti) counting system. The coincidence-noncoincidence approach enables us to improve the sensitivities of various elements and obtain additional elements such as Ho, Ga and Zn that are not accurately determined in normal Ge(Li) counting. This approach is particularly useful when a small size sample is involved. The details of our INAA procedure and the systematics of coincidence-noncoincidence counting are described in Laul and Rancitelli (1977) and Laul et al. (1978). Silicon was determined using the 14 MeV neutron activation facility of Dow Chemical at Midland, Michigan, whereas the remaining 33 elements were determined after irradiation at the Oregon State University (OSU) TRIGA reactor. In each irradiation, two Apollo .7 soils, 73121 and 75081, and the USGS standards BCR-1 (duplicate), GSP-1, and PCC-1, and Allende standard (USNM) were included as internal standards to check for systematic errors and to minimize geometry problem in the counting procedure.

MODAL AND MICROPROBE ANALYSES

The procedure used here for modal and microprobe analyses is the same as previously reported by Vaniman and Papike (1977b). Modal

petrography was based on optical characterization of polished thin sections. Microprobe analyses were obtained on an ARL-EMX SM automated microprobe with one semi-fixed (for silicon) and three positionable spectrometers. Data were reduced by applying the matrix correction procedure of Bence and Albee (1968).

PETROGRAPHY AND MINERALOGY

We have subdivided the drill core lithic fragments into three major categories: mare basalt, fused soil, and highland rocks. The fused soils (agglutinates and dark matrix breccias) include mixtures of highland and mare rock types; Taylor et al. (1978) indicate ∿30-50% highland material in agglutinate glasses of the A-17 drill core. In the discussion below we will deal with the highland and mare rocks, but not with the fused soil components.

MARE ROCK TYPES

Ilmenite Basalts. The ilmenite basalt category includes a variety of textures and a wide range in mineral chemistry. At least two magma types are represented:

1) The commonest high-Ti mare basalt is the Apollo17 olivine porphyritic to plagioclase poikilitic series. This magma series spans a range in texture and mineral chemistry from vitrophyres with olivine (Fo_{77-65}) + armalcolite + CrAl-spinel, to plagioclase poikilitic rocks with pyroxene + plagioclase + ilmenite + cristobalite. Olivines may be zoned from Fo_{77} to Fo_{60}; plagioclase compositions vary from $An_{88}Or_0$ to $An_{75}Or_4$. Poorly zoned high-Ca augites in olivine porphyritic vitrophyres have ∿9 wt% Al_2O_3 and ∿6 wt% TiO_2; pyroxene atomic Al/Ti ratios >2 reflect some Al in octahedral as well as tetrahedral

coordination. The more slowly cooled, coarse plagioclase-poikilitic basalts of this series have pyroxenes zoned to more Ca-poor augites with final development of Fe-rich rims. In the slowly cooled rocks the pyroxene Al/Ti ratio is fixed at 2 (essentially all Al in tetrahedral coordination).

2) A much rarer ilmenite basalt in the Apollo 17 core is diabasic/ophitic in texture. Pyroxene compositions are similar to those in the slowly cooled ilmenite basalt described above, but olivines may be more Fe-rich (Fo_{65-50}). The greatest difference in mineralogy between the diabasic/ophitic basalt and the other Apollo 17 high-Ti basalts is in feldspar composition; the diabasic/ophitic basalt has plagioclase more Ca-rich (An_{90-95}).

Very Low Ti (VLT) Basalt. This is a new mare basalt type first recognized in the Apollo 17 drill core by Vaniman and Papike (1977c) and Taylor et al. (1977b). Although VLT basalt is a minor core component ($\sim$ 0.1% of all lithic fragments), this lithic type is important in our discussion because the Apollo 17 drill core is the "type locality" for VLT basalt. Variants of this rock type have since been found at Mare Crisium (ref. Conference on Luna 24, 1977). The mineral chemistry of Apollo 17 VLT basalt is characterized by early crystallization of CrAl spinel rather than ilmenite, by calcic plagioclase (An_{93-85}), by olivine cores of high Mg content ($\sim Fo_{75}$), and pyroxene zonation from low-Ca pigeonite (Wo_7En_{20}) to Fe-rich augite rims. One of the most distinctive features of VLT mineralogy is an extremely high Al:Ti ratio ($\sim$10) in initial stages of pyroxene crystallization (Vaniman and Papike, 1977c).

HIGHLAND ROCK TYPES

The initial survey by LSPET (1973) emphasized two highland rock types, an anorthositic gabbro with plagioclase cumulate texture (e.g., 77017) and a KREEPy (low-K Fra Mauro) noritic rock type (e.g., 77135). The KREEPy rock type is represented by textural variants including poikilitic rocks (POIK), recrystallized noritic breccia (RNB) and feldspathic basalt (Bence et al., 1974).

Recrystallized Noritic Breccia (RNB) and Poikilitic Rocks (POIK). The RNB/POIK rocks have two pyroxenes + feldspar $\pm$ olivine $\pm$ ilmenite, Fe and FeS. Textures and mineralogy range from POIK melt rocks with lath-shaped feldspar chadacrysts in augite + pigeonite oikocrysts to RNB textures (annealed grain boundaries) with orthopyroxene + diopsidic augite. Feldspars range in composition from $An_{97}Or_0$ to $An_{88}Or_2$. Pyroxenes have Al/Ti ratios $\geq$ 2, and olivine compositions range from Fo_{90} to Fo_{70}.

Feldspathic Basalts. Feldspathic basalts are rare in the drill core (Table 1). The major-element and Ti-Al-Cr compositions of pyroxene, olivine and plagioclase in the feldspathic basalts are similar to the mineral compositions of RNB and POIK rocks. Pyroxene rims in feldspathic basalts may be more Fe-rich (Fe/(Fe + Mg) >0.45) than pyroxene in the RNB and POIK rocks.

Anorthositic Gabbro. The term "anorthositic gabbro" is used for rocks with the texture and mineral composition of 77017 (LSPET, 1973; McCallum et al., 1974). Anorthositic gabbros have large ($\sim$0.25-0.5mm) blocky feldspar grains ($An_{98}Or_0$ - $An_{94}Or_{0.5}$) enclosing beads or "necklaces" of olivine and surrounded by a mortar-like matrix of poikilitic Ca-poor pyroxenes and Ca-rich pyroxenes. The pyroxene Ca-Fe-Mg compositions

The data from continuous strings of polished thin sections are plotted in Figure 3. This type of data array can be compared directly with the INAA data displayed as a function of depth (ref. figures 6, 7, 8 and 11 in following sections of this paper). Particularly notable is the increase of DMB and agglutinate fragments above and below unit 2 (the coarse-grained, immature mare unit). Unit 2 is marked by an abundance of pyroxene fragments (pyroxene composes ∿50% of the common A-17 high-Ti mare basalts) as well as an abundance of high-Ti mare basalt lithic fragments. We note that the orange/black glasses (a high-Ti mare composition) increase in unit 3, below the predominantly mare soils. The increase of high-Ti mare glasses below the high-Ti mare unit may reflect either (1) the inversion of a stratigraphy in which orange/black glass overlay a crystalline mare unit, or (2) mixture of crystalline mare soil with a highland + high-Ti glass soil in unit 3. The presence of an inverted flap in the upper A-17 drill core has been proposed from studies of site geology (LSPET, 1973), core dissection (Duke and Nagle, 1974), track and thermoluminescence data (Crozaz and Plachy, 1976), petrographic data (Vaniman and Papike, 1977b and Taylor et al, 1977a) and I_s/FeO data (Morris et al., 1978). Further studies of the deeper drill core will resolve the question of whether the orange/black glass increase in unit 3 was delivered to the site with the overturned flap or mixed into the overturned flap as part of an underlying highland + high-Ti glass soil.

There is a pronounced increase of highland material with depth in unit 3. Figure 3 shows that in unit 3 highland components such as colorless glass, plagioclase and RNB + POIK increase with depth. Morris et al. (1978) show a continuous increase in I_s/FeO with depth

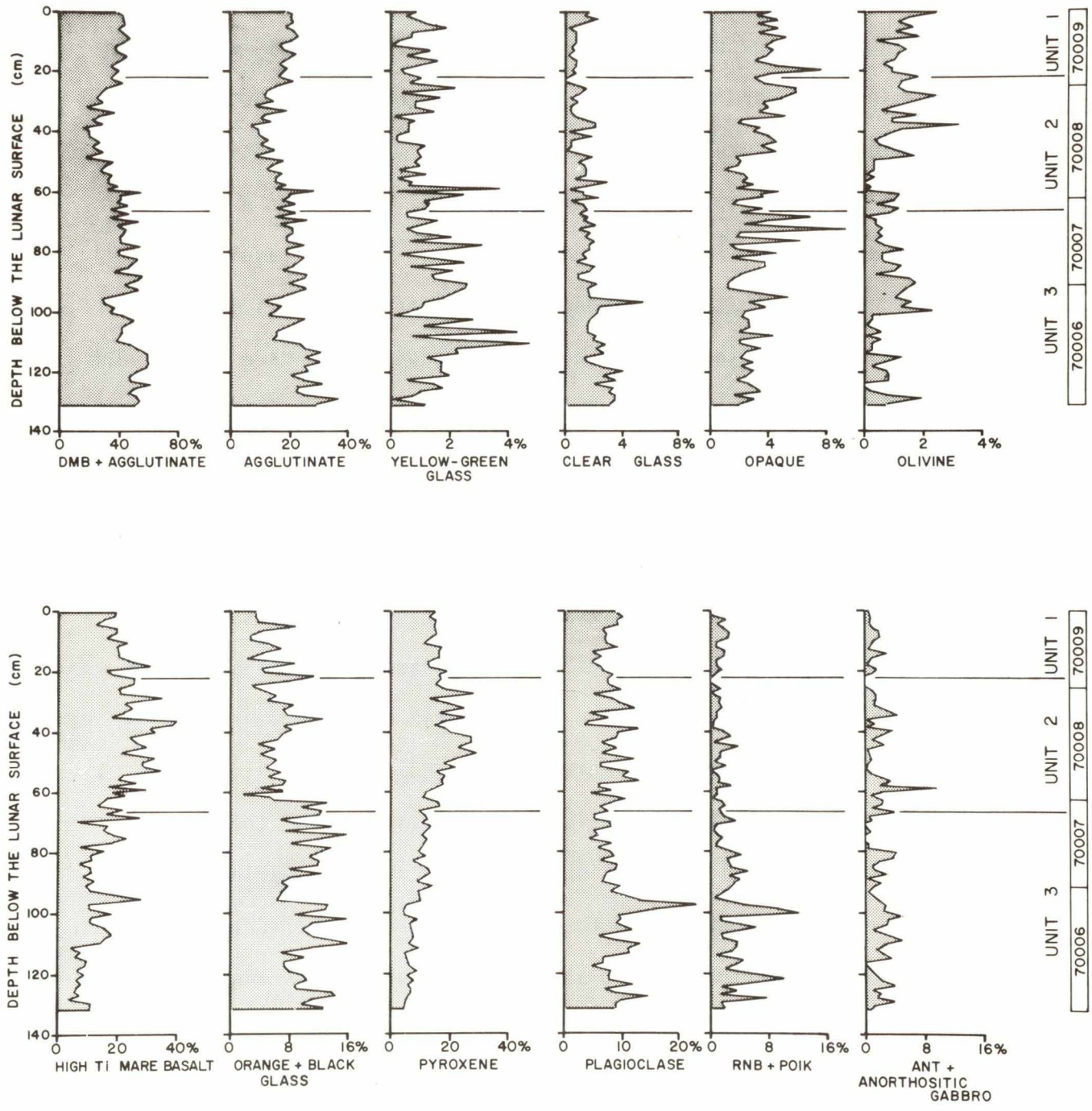

Figure 3. Stratigraphic distribution of lithic, mineral and glass components in core segments 70009-70006. Data are from polished thin sections; 0.02 to 2.0 clast data is normalized to 100%. Note that the horizontal scale varies between columns.

Table 2: Modal data from 0.02-0.09 mm and 0.09-1.0 mm grain mounts (each size range normalized to 100%)

	0.09-1.0 mm Grain Mounts	70009,432 70009,442	70009,433 70009,443	70009,434	70008,455 70008,467	70008,456 70008,468	70008,457 70008,469	70008,458 70008,470	70007,167 70008,414	70007,168 70007,415	70007,169 70007,416	70006,16 70006,301	70006,17 70006,302	70006,18 70006,303	70006,19 70006,304
	Depth	8.5 mm	93.5 mm	203.5 mm	280.5 mm	379.5 mm	470.5 mm	575.5 mm	706.5 mm	811.5 mm	896.5 mm	989.5 mm	1084.5 mm	1174.5 mm	1304.5 mm
	MARE BASALTS	19.75	12.40	15.44	26.41	41.58	28.06	20.35	16.17	18.13	11.05	14.56	9.52	4.20	15.47
	Highland Component														
	Anorthosite	---	---	0.19	---	---	---	1.10	2.45	2.93	3.40	---	1.83	1.68	2.38
	Norite/Troctolite	0.79	---	---	---	---	---	2.20	0.49	---	0.85	---	---	0.84	---
	LMB	0.79	0.62	0.57	---	1.89	2.76	1.10	1.96	2.93	5.10	5.82	2.19	3.36	2.38
	Feldspathic Basalt	---	---	0.19	---	1.89	---	---	---	0.59	0.85	---	1.10	1.68	2.38
	RNB/POIK	1.58	0.62	2.05	1.39	---	0.92	1.10	1.96	3.52	3.40	0.97	1.83	0.84	---
0.09 - 1.0 mm size fraction	*FUSED SOIL COMPONENT*														
	DMB	6.32	7.44	2.61	1.39	---	1.38	12.10	13.72	9.94	5.95	22.33	5.49	10.92	3.57
	Agglutinate	37.92	35.34	26.97	16.68	9.45	9.66	14.85	19.60	28.07	41.65	18.45	35.90	49.58	51.19
	MINERAL FRAGMENTS														
	Olivine	---	5.58	0.19	1.39	1.89	2.76	1.10	0.49	---	---	---	1.10	---	---
	Pyroxene	11.06	17.36	28.09	23.63	20.79	25.30	12.10	9.80	10.54	6.80	11.65	13.92	9.24	2.38
	Plagioclase	7.11	8.68	10.04	12.51	5.67	10.58	11.00	6.86	5.26	5.95	7.76	6.95	4.20	8.33
	Opaques	3.95	4.34	3.17	1.39	7.56	7.36	4.95	2.45	1.18	1.70	0.97	3.30	---	---
	GLASS FRAGMENTS														
	Orange/black *Yellow/green*	9.48	6.20	9.86	15.29	9.45	10.58	14.85	23.03	12.88	11.05	13.59	13.55	8.40	8.33
	Brown	---	1.24	---	---	---	---	---	---	---	---	---	0.37	---	---
	Gray	---	---	---	---	---	---	---	---	---	---	---	---	---	---
	Colorless	0.79	0.62	---	---	---	0.46	1.65	---	1.77	---	1.94	1.83	2.52	2.38
	OTHER COMPONENTS	---	---	0.38	---	---	0.46	1.65	0.98	2.34	1.70	1.94	1.11	2.52	1.19

	0.02-0.09 mm Grain Mounts	70009,436	70008,459	70008,460	70008,462	70008,464	70007,260	70007,261	70007,262	70006,183	70006,184	70006,185	70006,186
	Depth	93.5 mm	280.5 mm	379.5 mm	470.5 mm	575.5 mm	706.5 mm	811.5 mm	896.5 mm	989.5 mm	1084.5 mm	1174.5 mm	1304.5 mm
	MARE BASALTS	8.0	12.3	10.2	8.7	19.5	16.1	13.2	9.0	11.0	6.7	5.1	3.3
	Highland Component												
	Anorthosite	0.1	0.3	---	0.6	0.7	0.9	1.2	1.3	1.1	1.1	0.4	0.5
	Norite/Troctolite	---	---	---	---	---	0.1	---	---	---	---	0.2	---
	LMB	0.9	0.2	0.2	0.5	1.1	1.2	0.6	1.3	1.9	0.7	0.3	---
	Feldspathic Basalt	---	---	---	---	0.1	---	---	---	---	---	0.1	---
	RNB/POIK	1.5	0.6	0.5	1.0	0.2	0.9	0.6	0.6	0.4	1.0	0.5	0.1
0.02 - 0.09 mm size fraction	*FUSED SOIL COMPONENT*												
	DMB	13.9	7.8	5.3	7.2	9.7	15.6	9.3	9.1	14.2	13.8	23.7	24.2
	Agglutinate	18.8	8.1	11.4	12.2	12.7	14.5	11.7	19.3	16.1	22.1	14.8	23.0
	MINERAL FRAGMENTS												
	Olivine	0.1	0.1	0.3	0.5	0.2	0.3	0.6	0.4	0.1	1.0	1.3	1.5
	Pyroxene	17.1	16.2	26.3	24.3	25.0	13.3	18.2	17.7	21.0	14.1	22.6	19.2
	Plagioclase	19.4	23.7	15.1	13.4	7.0	13.0	12.0	15.1	12.0	20.4	10.5	10.4
	Opaques	7.3	9.9	9.7	9.8	5.8	5.1	6.9	4.2	5.2	4.2	2.8	3.5
	GLASS FRAGMENTS												
	Orange/black *Yellow/green*	9.8	17.4	18.2	19.6	9.7	11.1	12.1	14.5	12.4	9.1	13.1	6.5
	Brown	0.4	0.6	0.1	---	0.7	1.2	2.8	1.3	1.4	0.6	1.4	2.0
	Gray	0.2	0.1	0.1	---	2.0	0.2	0.3	0.1	---	0.1	---	0.2
	Colorless	2.1	2.3	2.1	1.5	4.7	6.3	9.6	4.7	2.9	4.4	2.8	5.5
	OTHER COMPONENTS	0.4	0.4	0.5	0.7	0.9	0.2	0.9	0.8	0.3	0.7	---	0.2

in 70007 (upper unit 3) which reflects an inhomogeneous but monotonically increasing mixture of mature highland soils with a corresponding decrease in immature mare soils.

Modal data were also obtained from polished grain mounts. The grain mounts were made from 20-90 μm and >90 μm soil splits taken from each of the 14 soil allocations which were sieved and analyzed by INAA. Data from the polished grain mounts are summarized in Table 2. These data can be correlated directly with the 20-90 μm and >90 μm soil analyses reported below. There is some advantage in having grain mounts from each soil analyzed, but we have found in this study that the grain mounts are less reliable for modal analysis because section thickness is irregular, making the identification of colored grains difficult in plane polarized light and identification of anisotropic grains difficult in cross-polarized light. One of the most critical problems is the identification of glass color types in abnormally thin sections (<30 μm thick) where orange and yellow glasses cannot be distinguished. For this reason, much of the glass data in table 2 has been grouped into a broader category: (orange/black + yellow/green).

STRATIGRAPHY OF MINERAL COMPOSITIONS

Some features of major- and minor-element mineral chemistry can be used to distinguish between possible mare and highland sources. Figures 4-5 show variation in mineral composition (feldspar Ab-An-Or and pyroxene Ca-Mg-Fe) at six levels within core segments 70006-70009. At each of the six levels an area of ∿10 mm^2 was selected; within each of these areas all feldspar, pyroxene and olivine grains were analyzed. Several analyses were made within each pyroxene grain to

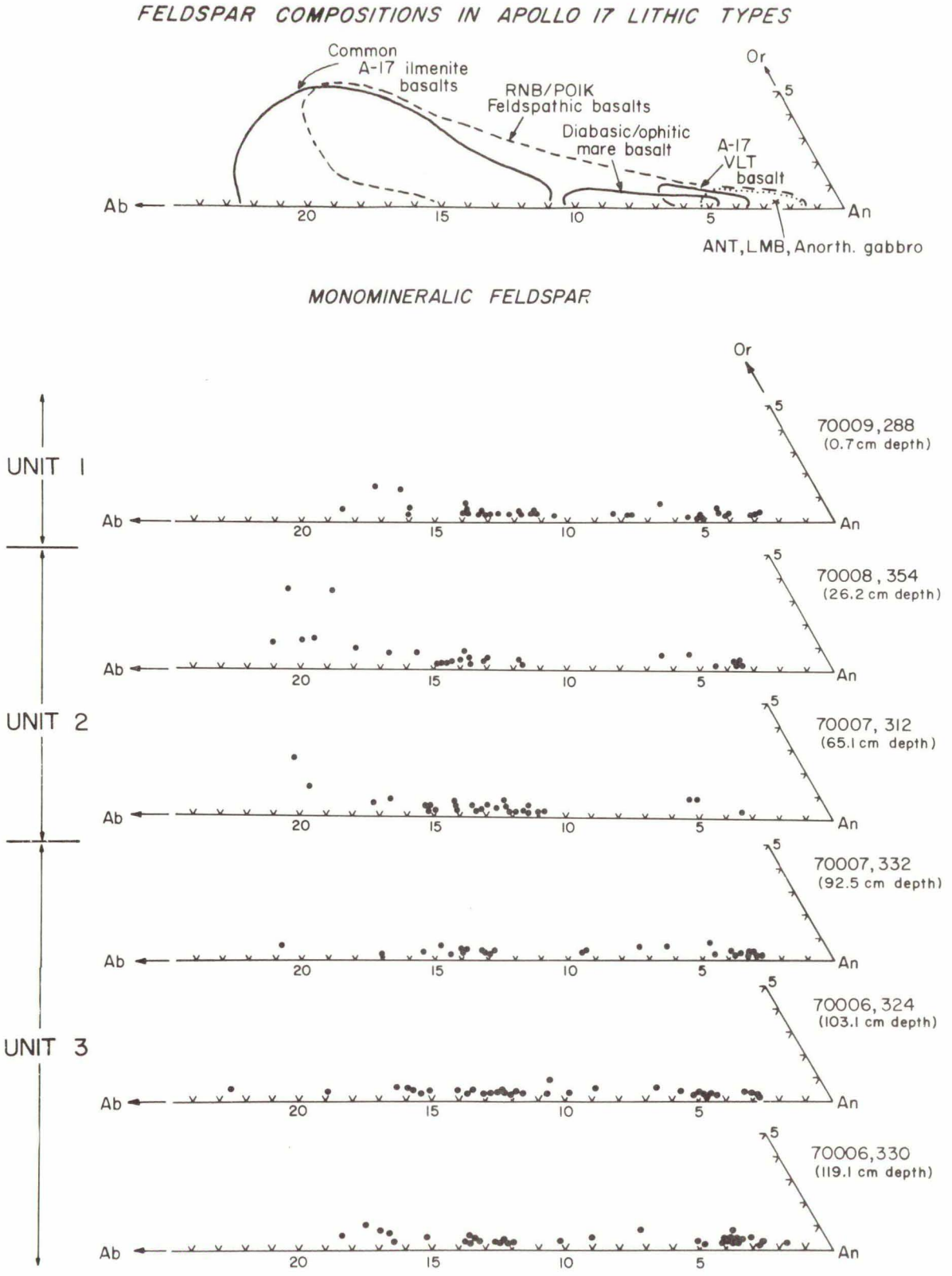

Figure 4. Feldspar compositional data. The uppermost diagram shows the ranges of feldspar composition in Apollo 17 lithic types; lower six diagrams show the stratigraphy of feldspar mineral fragment compositions in six levels of 70009-70006.

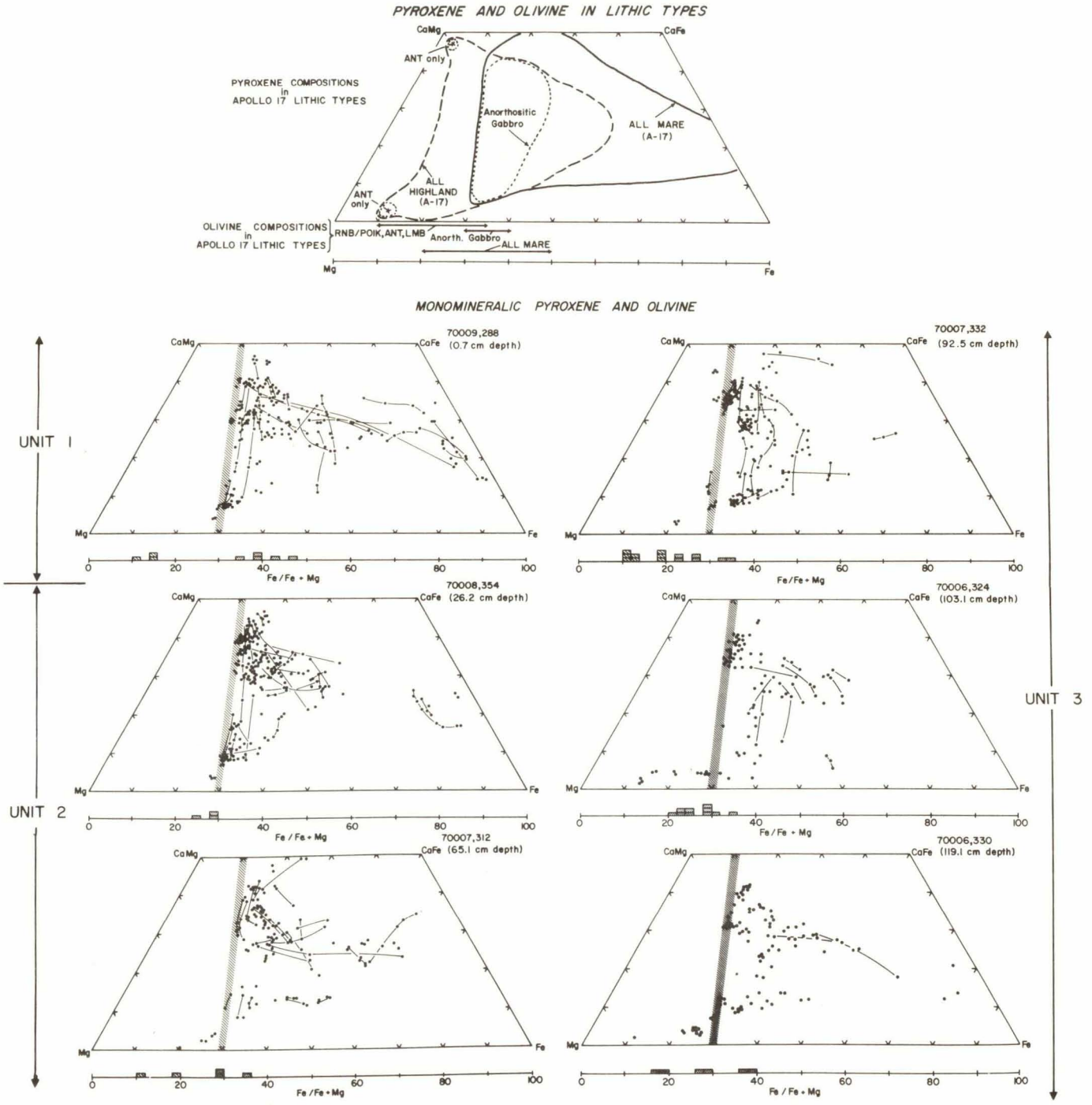

Figure 5. Pyroxene and olivine compositional data. The uppermost diagram shows the ranges of pyroxene and olivine composition in Apollo 17 lithic types. Note that low-Ca pyroxenes more magnesian than En_{70} come from highland rather than mare sources, and olivines more magnesian than Fo_{80} come from highland sources. The lower six diagrams show the stratigraphy of pyroxene and olivine mineral fragments in six levels of 70009-70006.

account for zonation. At the top of each figure (4-5) is a summary diagram showing the mineral composition fields of different rock types. These two figures point out several important conclusions regarding source-rock petrology:

1) The common high-Ti Apollo 17 basalts have feldspars less calcic than An_{88}. Concentrations of these relatively Ca-poor feldspars are seen in unit 2 (Figure 4). Other mare basalts (VLT and diabasic-ophitic) have feldspars that are more calcic, but these other mare rocks are rare (Table 1). Therefore, it is reasonable to assume that most feldspar grains more calcic than An_{88} are from highland source rocks. Such calcic feldspars are concentrated in units 1 and 3.

2) Olivines more Mg-rich than Fo_{80} and low-Ca pyroxenes more Mg-rich than En_{70} are derived from highland sources (Figure 5). There is a marked increase of Fo_{80-90} olivine and low-Ca pyroxene with Mg $>En_{70}$ in unit 3, below the coarse-grained unit. This corresponds with the well-documented increase of highland components below the coarse unit (Duke and Nagle, 1974). However, the nature of the highland component is not the same in all levels of unit 3. Note that the increased highland component is represented by Mg-rich olivine in 70007, 332 but Mg-rich pyroxene is dominant in 70006. These highland mineral types could represent one or several rock types (ANT, LMB, POIK/RNB, feldspathic basalt or spinel cataclasite). However, the evidence for an increased KREEPy component in all soils of 70006 (discussion of INAA data below) as well as the modal data indicating an increase of KREEP-bearing POIK in 70006 suggest that POIK rocks account for a significant amount of the increase highland component.

CHEMICAL SYSTEMATICS

RESULTS

The data for 34 major-, minor- and trace-elements determined by INAA in 48 bulk soils and size fractions (each 4-30 mg) are presented in Tables 3 to 6 along with controls 73121, 75081 and (USGS) BCR-1. Tables 3 and 4 list the major- and minor-element abundances whereas Tables 5 and 6 contain trace-element abundances. In cases where the actual bulk samples were analyzed, these are compared with the calculated bulk values to test the mass balance. Overall, the agreement between the actual and calculated bulk soil compositions is remarkably good for both major- and trace-elements. The only exception we note is in sample 70008,456 (38 cm depth) where the mass balance is poor for trace elements. The calculated bulk LIL (Ba, Sr, REE, Hf, Th, etc.) and K_2O abundances are ~30% higher than the actual bulk analyses (Table 3).

For SiO_2, FeO, Sc, Co, Hf, Ta and Zn, we used (USGS) BCR-1 values as an internal standard. These values are listed in Tables 4 and 6 and the agreement with the recommended values of Flanagan (1973) is excellent. For Th, we used GSP-1 = 105 ppm. For Au, Ir and Ni, we used the Allende standard (USNM) analyzed by E. Anders' group (Takahashi et al., 1978). Their mean values for six replicates are Au = 0.140 ppm; Ir = 0.780 ppm; and Ni = 14200 ppm, respectively. Unfortunately, our Ni and possible Au and Ir values especially in the <20 μm fractions are highly suspect because of possible Ni contamination from abrasion of the sieves. Au and Ir may also be carried as imporities with Rh and Ni from the sieves. Thus, any interpretation of the metoeritic component using these siderophile elements should be made with caution.

TABLE 3. MAJOR AND MINOR ABUNDANCES (%) VIA INAA IN BULK AND SIZE FRACTIONS OF 70009 AND 70008 CORES

SAMPLE (DEPTH)	SIZE (μm)	WEIGHT FRACTION	WEIGHT (mg)	SiO_2	TiO_2	Al_2O_3	FeO	MgO	CaO	Na_2O	K_2O	MnO	Cr_2O_3	TOTAL
70009,432	BULK	---	16.8	40.4	8.3	12.1	17.1	10.7	10.8	0.39	0.085	0.224	0.410	100.5
PARENT 9	CALCULATED			40.3	8.2	12.3	17.1	10.6	11.1	0.40	0.094	0.220	0.417	100.7
0.6 - 1.1 cm	>90	0.418	21.0	39.8	8.2	12.1	16.9	10.2	11.8	0.40	0.086	0.226	0.407	100.1
	20-90	0.390	20.1	40.8	8.5	11.7	17.4	11.4	10.4	0.40	0.090	0.223	0.430	101.3
	<20	0.192	10.4	40.5	7.4	14.2	16.9	9.6	11.1	0.41	0.12	0.191	0.413	100.8
70009,433	>90	0.441	30.0	40.8	8.9	10.7	17.4	9.9	10.8	0.38	0.092	0.234	0.427	99.6
PARENT 45	20-90	0.390	26.8	40.8	8.6	12.2	17.5	10.6	11.3	0.39	0.086	0.222	0.417	102.1
9.1 - 9.6 cm	<20	0.169	12.5	42.2	7.8	14.3	15.5	8.4	10.7	0.42	0.12	0.183	0.400	100.0
70009,434	BULK	---	3.65	40.7	8.5	11.5	17.5	10.0	10.0	0.41	0.085	0.224	0.420	99.4
PARENT 99	CALCULATED			40.8	8.6	11.5	17.4	10.3	10.1	0.41	0.091	0.227	0.407	99.8
20.1 - 20.6 cm	>90	0.445	28.0	40.4	8.7	10.9	18.0	10.2	10.4	0.41	0.081	0.230	0.430	99.7
	20-90	0.354	21.7	40.4	8.9	11.1	17.6	11.0	9.8	0.40	0.094	0.238	0.400	99.9
	<20	0.201	12.8	42.3	7.8	13.4	15.5	9.4	10.0	0.43	0.11	0.202	0.370	99.5
70008,455	>90	0.579	41.0	39.9	9.8	10.0	18.3	9.0	10.9	0.40	0.078	0.240	0.400	99.0
PARENT 153	20-90	0.286	20.3	40.1	9.0	10.4	19.2	10.3	10.6	0.40	0.089	0.247	0.460	100.8
27.8 - 28.3 cm	<20	0.135	9.08	41.1	7.6	12.7	16.8	9.6	10.9	0.52	0.13	0.201	0.470	100.0
70008,456	BULK	---	5.89	39.5	9.1	11.1	18.3	9.6	11.2	0.43	0.068	0.230	0.460	100.0
PARENT 110	CALCULATED			40.2	9.0	10.9	18.4	9.6	11.0	0.43	0.089	0.232	0.450	100.2
37.7 - 38.2 cm	>90	0.474	28.7	39.9	9.6	10.4	18.7	9.3	10.8	0.40	0.078	0.240	0.440	99.9
	20-90	0.336	20.3	39.9	8.9	10.5	19.2	10.3	11.1	0.43	0.082	0.240	0.470	101.3
	<20	0.190	12.5	41.7	7.4	12.6	16.2	9.0	11.1	0.49	0.13	0.199	0.420	99.2
70008,457	>90	0.439	29.4	40.6	8.5	11.0	17.5	9.0	11.5	0.40	0.12	0.238	0.410	99.3
PARENT 72	20-90	0.367	23.8	40.5	8.6	10.6	19.0	10.7	10.9	0.42	0.095	0.233	0.450	101.5
46.8 - 47.3 cm	<20	0.194	13.2	41.4	7.3	12.7	17.3	9.1	10.1	0.50	0.14	0.205	0.455	99.2
70008,458	>90	0.453	23.5	40.6	7.7	10.9	18.0	10.2	11.2	0.41	0.085	0.232	0.470	99.8
PARENT 30	20-90	0.390	21.4	40.8	7.5	11.4	18.2	10.8	10.0	0.41	0.094	0.236	0.450	99.9
57.3 - 57.8 cm	<20	0.157	7.37	42.5	7.0	13.5	16.5	9.7	11.1	0.50	0.13	0.200	0.470	101.6

TABLE 4. MAJOR AND MINOR ABUNDANCES (%) VIA INAA IN BULK AND SIZE FRACTIONS OF 70007 AND 70006 CORES

SAMPLE (DEPTH)	SIZE (μm)	WEIGHT FRACTION	WEIGHT (mg)	SiO_2	TiO_2	Al_2O_3	FeO	MgO	CaO	Na_2O	K_2O	MnO	Cr_2O_3	TOTAL
70007,167	BULK	---	4.03	41.8	6.8	12.3	17.9	11.0	10.0	0.42	0.11	0.225	0.480	101.0
PARENT 120	CALCULATED			41.6	6.7	12.1	17.7	10.9	10.5	0.42	0.10	0.222	0.463	100.7
70.4 - 70.9 cm	>90	0.372	20.5	41.7	7.0	11.6	18.2	10.7	10.4	0.41	0.085	0.226	0.470	100.8
	20-90	0.428	25.6	41.5	6.7	11.6	17.7	11.3	10.3	0.40	0.10	0.227	0.450	100.3
	<20	0.200	11.1	41.6	6.2	14.1	16.8	10.3	10.9	0.48	0.15	0.206	0.480	101.2
70007,168	>90	0.366	22.0	41.7	6.0	13.9	15.9	10.1	11.3	0.39	0.087	0.206	0.440	100.0
PARENT 58	20-90	0.450	27.0	41.8	5.8	12.5	17.2	11.0	11.0	0.39	0.099	0.217	0.420	100.4
80.9 - 81.4 cm	<20	0.184	10.6	41.7	5.8	15.0	15,7	9.4	11.7	0.46	0.13	0.188	0.440	100.5
70007,169	>90	0.415	23.1	42.5	5.0	14.2	15.3	9.9	12.2	0.44	0.12	0.192	0.345	100.2
PARENT 24	20-90	0.386	21.9	42.3	5.7	12.7	15.9	11.0	11.1	0.38	0.10	0.199	0.380	99.8
89.4 - 89.9 cm	<20	0.199	11.9	42.5	5.3	15.3	14.8	9.1	11.4	0.46	0.13	0.183	0.405	99.6
70006,16	>90	0.351	23.4	42.2	6.0	13.4	16.0	10.0	11.0	0.41	0.10	0.205	0.405	99.7
PARENT 36	20-90	0.434	28.4	42.5	5.7	12.8	16.0	10.7	10.9	0.39	0.10	0.212	0.380	99.7
97.7 - 98.2 cm	<20	0.215	14.0	43.1	5.4	15.2	14.4	9.8	11.5	0.45	0.14	0.188	0.390	100.6
70006,17	BULK	---	5.38	42.1	6.1	13.0	16.3	10.1	10.5	0.43	0.11	0.200	0.450	99.3
PARENT 79	CALCULATED			42.4	6.1	12.7	16.2	10.3	10.9	0.43	0.11	0.210	0.430	99.8
108.2 - 108.7 cm	>90	0.407	20.2	42.3	6.3	12.1	16.5	10.1	10.8	0.43	0.10	0.213	0.410	99.3
	20-90	0.400	20.5	42.1	6.0	12.3	16.5	10.6	10.9	0.41	0.10	0.218	0.450	99.6
	<20	0.193	9.48	43.3	5.7	14.7	15.0	9.9	11.0	0.46	0.16	0.188	0.430	100.8
70006,18	>90	0.324	19.7	42.0	5.6	13.7	15.8	10.3	11.7	0.39	0.096	0.207	0.430	100.2
PARENT 116	20-90	0.451	29.9	42.7	5.1	13.6	15.6	10.5	11.6	0.41	0.10	0.202	0.370	100.2
117.2 - 117.7 cm	<20	0.225	13.9	42.8	5.4	15.8	14.2	10.0	11.5	0.42	0.14	0.185	0.390	100.8
70006,19	BULK	---	9.31	42.6	5.5	14.0	15.6	10.0	11.7	0.42	0.12	0.200	0.415	100.5
PARENT 167	CALCULATED			42.5	5.6	14.3	15.6	10.2	11.7	0.41	0.12	0.198	0.413	101.0
130.2 - 130.7 cm	>90	0.309	17.8	42.6	5.8	13.8	15.8	9.8	11.9	0.42	0.095	0.205	0.430	100.8
	20-90	0.407	24.9	42.2	5.5	13.7	16.2	10.9	11.7	0.40	0.10	0.203	0.410	101.3
	<20	0.284	16.5	42.8	5.4	15.7	14.6	9.8	11.5	0.42	0.16	0.183	0.400	101.0
CONTROLS														
73121,17				45.4	1.4	20.6	8.5	10.0	13.1	0.39	0.14	0.110	0.210	99.9
75081,21				40.4	9.1	11.1	17.3	9.6	10.9	0.44	0.080	0.230	0.430	99.6
BCR-1				≡ 54.5	2.2	13.6	≡ 12.2	3	6.95	3.20	1.70	0.180	0.0025	---

ESTIMATED ERRORS BASED ON COUNTING STATISTICS ARE: ±0.5 - 3% FOR SiO_2, TiO_2, Al_2O_3, FeO, MnO, Na_2O AND Cr_2O_3; ±5% FOR MgO, CaO AND K_2O.

TABLE 5. TRACE ABUNDANCES VIA INAA IN BULK AND SIZE FRACTIONS OF 70009 AND 70008 CORES (ALL VALUES IN ppm UNLESS NOTED)

SAMPLE (DEPTH)	SIZE (μm)	WEIGHT FRACTION	Sc	V	Co	Ba	Sr	La	Ce	Nd	Sm	Eu	Tb	Dy	Ho	Yb	Lu	Hf	Ta	Th	U	Ga	Zn	Au (ppb)	Ni*	Ir (ppb)
70009, 432	BULK	---	56.6	100	32.3	120	210	7.90	28	23	8.06	1.76	1.9	11.4	2.9	7.11	1.07	6.60	1.20	0.95	0.23	6.3	44	3	150	<10
PARENT 9	CALCULATED		57.6	95	35.5	120	200	8.08	29	23	8.10	1.82	1.9	11.9	2.8	7.11	1.06	6.50	1.23	1.08	0.26	6.6	46	---	---	---
0.6 - 1.1 cm	>90	0.418	61.4	100	28.8	130	190	7.27	27	22	7.71	1.80	1.9	11.7	2.8	7.40	1.10	6.42	1.13	0.96	0.20	5.4	32	3	120	<10
	20-90	0.390	58.9	90	39.7	100	190	7.53	28	22	7.97	1.70	2.0	12.1	2.8	7.00	1.06	6.52	1.20	0.98	0.23	6.2	40	3	200	12
	<20	0.192	46.8	90	41.7	120	250	11.0	36	26	9.20	2.10	2.0	12.1	2.7	6.70	0.99	6.47	1.50	1.55	0.45	9.8	88	20	580	25
70009, 433	>90	0.441	67.0	90	31.4	110	180	7.67	26	22	8.10	1.78	2.0	12.4	2.8	6.89	1.00	7.21	1.35	0.94	0.24	6.4	30	2	140	<10
PARENT 45	20-90	0.390	58.7	90	32.5	110	180	7.84	27	24	8.00	1.84	2.0	11.3	2.7	6.71	1.00	6.33	1.28	1.05	0.25	5.6	38	3	240	12
9.1 - 9.6 cm	<20	0.169	43.0	90	38.2	130	200	11.5	39	26	8.66	2.00	2.1	11.8	2.5	6.10	0.90	6.70	1.35	1.90	0.55	9.5	80	16	600	30
70009, 434	BULK	---	60.0	100	34.9	110	180	8.30	29	25	8.80	1.90	2.1	12.5	2.8	7.40	1.10	6.60	1.35	0.94	---	---	40	2	100	<10
PARENT 99	CALCULATED		58.7	95	34.0	105	185	8.58	30	24	8.80	1.86	2.1	12.3	2.9	7.12	1.06	6.40	1.29	0.97	0.28	6.8	49	---	---	---
20.1 - 20.6 cm	>90	0.445	65.0	100	35.5	95	180	7.60	30	24	9.34	1.93	2.3	13.2	3.0	8.00	1.17	6.84	1.40	0.94	0.24	5.4	35	3	220	12
	20-90	0.354	60.6	90	32.1	110	190	9.00	30	24	8.32	1.72	2.0	12.0	2.9	6.65	1.00	5.81	1.15	0.83	0.29	6.8	40	2	140	<10
	<20	0.201	41.6	90	34.1	120	190	10.0	31	26	8.44	1.95	1.9	11.0	2.7	6.01	0.91	6.43	1.30	1.30	0.34	10	95	(30)	440	30
70008, 455	>90	0.579	72.1	100	22.3	100	160	6.54	25	24	8.50	1.75	2.2	12.6	2.6	8.21	1.16	6.50	1.44	0.40	---	5.2	30	---	60	<10
PARENT 153	20-90	0.286	62.5	100	35.4	110	150	7.28	27	25	8.80	1.91	2.1	12.3	2.9	7.61	1.10	6.54	1.30	0.60	---	6.3	45	3	220	<15
27.8 - 28.3 cm	<20	0.135	44.5	95	36.6	150	200	9.48	31	26	8.49	1.97	2.0	10.6	2.6	6.32	0.93	6.10	1.37	1.10	0.4	14	150	(70)	600	40
70008, 456	BULK	---	63.6	100	28.4	80	150	5.40	20	19	6.30	1.70	1.8	10.0	2.5	6.64	0.95	5.56	1.30	0.60	---	9.0	40	2	110	<10
PARENT 110	CALCULATED		59.2	97	31.8	120	190	7.57	26	24	8.42	1.88	2.1	12.4	2.8	7.50	1.06	6.72	1.24	0.78	---	9.5	67	---	---	---
37.7 - 38.2 cm	>90	0.474	64.6	100	27.4	120	210	6.81	25	23	8.10	1.77	2.2	13.0	2.7	7.70	1.10	6.74	1.20	0.60	---	9.0	50	3	200	<15
	20-90	0.336	60.8	90	35.5	110	170	7.50	28	25	8.78	1.90	2.2	12.3	3.0	7.80	1.10	7.12	1.30	0.80	0.3	6.6	50	3	350	<15
	<20	0.190	43.0	100	36.1	140	180	9.60	28	26	8.59	2.05	1.9	11.3	2.6	6.50	0.93	6.00	1.25	1.20	0.4	16	140	(100)	410	25
70008, 457	>90	0.439	68.8	100	23.5	120	150	6.96	27	23	8.80	1.85	2.2	14.0	2.8	8.00	1.10	7.10	1.40	0.50	---	6.4	40	2	150	<10
PARENT 72	20-90	0.367	61.5	90	35.8	110	140	7.70	28	24	8.50	1.90	2.1	12.0	2.7	7.52	1.06	6.75	1.40	0.70	---	6.4	60	---	710	30
46.8 - 47.3 cm	<20	0.194	47.9	85	38.5	110	200	10.5	36	29	9.46	2.10	2.1	12.0	2.6	6.46	0.97	6.58	1.40	1.40	0.4	15	160	17	1100	50
70008, 458	>90	0.453	65.0	110	32.4	90	160	7.67	27	23	8.17	1.72	2.1	12.1	3.0	7.48	1.05	6.58	1.35	0.85	---	6.4	40	2	150	<10
PARENT 30	20-90	0.390	54.9	90	38.5	110	170	7.70	29	22	7.62	1.76	1.9	11.0	2.7	7.03	0.98	6.58	1.10	1.10	0.3	7.8	60	3	150	<10
57.3 - 57.8 cm	<20	0.157	42.9	85	40.7	130	210	10.1	31	24	7.82	1.90	2.0	10.4	2.4	5.85	0.87	6.40	1.28	1.30	0.4	12	130	5.0	290	15

TABLE 6. TRACE ABUNDANCES VIA INAA IN BULK AND SIZE FRACTIONS OF 70007 AND 70006 CORES (ALL VALUES IN ppm UNLESS NOTED)

SAMPLE (DEPTH)	SIZE (μm)	WEIGHT FRACTION	Sc	V	Co	Ba	Sr	La	Ce	Nd	Sm	Eu	Tb	Dy	Ho	Yb	Lu	Hf	Ta	Th	U	Ga	Zn	Au (ppb)	Ni*	Ir (ppb)
70007,167	BULK	---	50.0	95	37.5	100	180	8.60	26	20	7.20	1.72	1.9	10.3	2.4	6.10	0.90	6.10	1.10	1.10	0.3	9.0	60	2	150	<10
PARENT 120	CALCULATED		52.0	97	38.3	110	180	9.24	29	22	7.39	1.71	2.0	11.0	2.7	6.36	0.92	6.12	1.10	1.25	0.4	9.1	70	---	---	---
70.4 - 70.9 cm	>90	0.372	60.0	95	35.0	90	180	9.30	30	24	7.70	1.80	2.2	12.0	2.9	7.20	1.05	6.70	1.11	1.30	0.4	8.5	40	3	120	<10
	20-90	0.428	50.1	100	38.9	120	180	8.57	27	20	7.10	1.60	1.8	10.5	2.6	6.05	0.85	5.60	1.00	1.10	0.4	7.8	65	3	180	<10
	<20	0.200	41.2	95	43.4	120	170	10.6	31	23	7.44	1.78	1.9	10.3	2.4	5.50	0.81	6.20	1.10	1.50	0.4	13	140	7.0	400	20
70007,168	>90	0.366	49.3	85	31.8	100	170	6.65	23	18	6.30	1.55	1.6	9.6	2.4	6.00	0.84	5.45	1.20	0.95	---	5.5	40	2	150	<10
PARENT 58	20-90	0.450	50.5	85	39.0	100	160	8.46	26	21	7.00	1.60	1.7	10.4	2.6	6.10	0.85	6.00	1.00	1.05	0.4	6.7	60	3	210	<15
80.9 - 81.4 cm	<20	0.184	39.7	85	41.0	110	210	10.7	31	23	7.25	1.70	2.0	10.1	2.4	5.70	0.84	6.10	1.20	1.60	0.48	12	100	7.2	600	26
70007,169	>90	0.415	46.4	80	49.0	150	160	10.7	36	28	8.20	1.60	1.9	11.4	2.8	7.00	1.00	6.60	1.15	1.60	0.40	6.7	40	6.0	430	20
PARENT 24	20-90	0.386	47.0	80	36.7	120	170	8.50	27	20	6.71	1.48	1.6	9.9	2.3	5.90	0.83	5.70	1.15	1.25	0.35	7.5	50	3	270	<15
89.4 - 89.9 cm	<20	0.199	37.6	90	41.0	160	190	11.4	33	24	7.33	1.70	1.7	9.7	2.5	5.60	0.85	5.90	1.14	1.75	0.50	10	90	14	710	50
70006,16	>90	0.351	53.0	80	37.5	130	180	9.00	28	20	6.92	1.60	1.6	9.7	2.4	6.10	0.85	5.60	1.00	1.20	0.4	7.1	45	3	290	15
PARENT 36	20-90	0.434	47.9	85	35.4	110	160	9.15	28	21	7.20	1.48	1.7	10.6	2.4	6.36	0.92	5.70	0.95	1.30	0.40	6.0	45	3	250	<15
97.7 - 98.2 cm	<20	0.215	36.7	80	39.7	190	170	12.3	38	26	8.38	1.70	1.8	11.0	2.4	5.91	0.90	6.11	1.00	2.05	0.5	10	80	(70)	550	25
70006,17	BULK	---	50.0	90	36.9	120	190	9.36	28	23	7.15	1.70	1.9	10.0	2.4	6.10	0.90	6.00	1.05	1.35	0.4	6.6	40	3	220	<15
PARENT 79	CALCULATED		50.2	95	36.2	120	180	9.50	29	23	7.38	1.63	1.8	10.5	2.5	6.25	0.93	5.80	1.02	1.40	0.4	6.4	46	---	---	---
108.2 - 108.7 cm	>90	0.407	54.9	100	31.9	130	160	8.18	28	22	7.22	1.60	1.7	10.2	2.5	6.38	0.95	5.79	1.10	1.25	0.4	5.0	35	3	170	<10
	20-90	0.400	50.4	90	38.6	100	190	9.52	29	23	7.30	1.60	1.9	10.8	2.6	6.25	0.92	5.64	0.95	1.30	0.4	6.0	40	4	640	15
	<20	0.193	39.8	90	40.5	130	190	12.3	34	25	7.90	1.77	2.0	10.6	2.5	6.00	0.89	6.02	1.00	1.80	0.50	10	80	18	970	30
70006,18	>90	0.324	51.9	100	38.5	130	150	8.50	26	20	6.43	1.56	1.7	9.4	2.3	5.54	0.83	5.45	0.92	1.30	0.4	6.0	40	3	250	<15
PARENT 116	20-90	0.451	48.1	95	36.0	120	160	8.86	27	21	6.76	1.51	1.6	10.0	2.4	5.99	0.87	5.52	1.00	1.30	0.4	6.3	45	3	250	<15
117.2 - 117.7 cm	<20	0.225	37.7	80	39.0	130	160	11.7	34	23	7.37	1.66	1.9	11.4	2.6	5.90	0.84	5.80	1.10	1.90	0.55	8.0	60	9.5	420	25
70006,19	BULK	---	47.0	90	35.7	130	160	11.0	33	24	7.60	1.58	2.0	10.3	2.6	6.29	0.94	5.73	1.00	1.50	0.5	6.1	40	7.0	260	17
PARENT 167	CALCULATED		45.5	90	37.2	120	150	10.1	30	23	7.10	1.55	1.8	10.4	2.4	6.06	0.87	5.82	0.97	1.50	0.4	6.5	48	---	---	---
130.2 - 130.7 cm	>90	0.309	48.1	90	32.8	120	120	10.0	27	24	7.00	1.46	2.0	11.0	2.5	6.17	0.91	5.50	0.85	1.40	0.4	6.0	35	3	240	<15
	20-90	0.407	49.2	95	37.8	120	140	9.40	29	22	7.17	1.55	1.6	9.8	2.5	6.36	0.88	6.01	0.92	1.30	0.4	5.2	40	3	270	<15
	<20	0.284	37.5	80	41.2	130	190	11.2	33	23	7.00	1.64	1.9	10.6	2.2	5.51	0.81	5.90	1.16	1.90	0.50	9.0	75	7.7	520	30
CONTROLS																										
73121,17			18.3	50	31.0	170	160	15.1	38	26	7.20	1.30	1.5	9.2	2.2	5.40	0.76	5.50	0.73	2.90	0.85	6.0	20	4	330	16
75081,21			67.0	100	30.0	100	160	7.70	28	25	8.40	1.80	2.1	13.0	3.0	7.40	0.98	7.40	1.40	0.90	0.25	6.4	35	---	110	<10
BCR-1			≡32.0	410	≡36.0	670	330	25.5	54	30	6.70	2.00	1.0	6.3	1.3	3.40	0.53	≡4.70	≡0.80	6.0	1.7	24	≡130	---	---	---

ESTIMATED ERRORS BASED ON COUNTING STATISTICS ARE: ± 0.5 - 3% FOR Sc, Co, La, Sm, Eu, Yb AND Lu; ± 5% FOR V, Tb, Dy, Hf AND Ta; ± 5 - 10% FOR Ba, Ce, Nd, Ho, Th, Ga, Zn AND Ni; ± 10 - 20% FOR Sr, U, Au AND Ir. THE UPPER LIMITS ARE BASED ON 3σ OF THE PEAK AREA. THE VALUES IN PARENTHESIS ARE SUSPECT OF CONTAMINATION.

* THE Ni, Au AND Ir VALUES ARE HIGHLY SUSPECT OF CONTAMINATION FROM THE Rh-PLATED Ni SIEVES.

Typical errors in our INAA procedure based on counting statistics using BCR-1 and other controls are: ± 0.5 - 3% for SiO_2, TiO_2, Al_2O_3, FeO, MnO, Na_2O, Cr_2O_3, Sc, Co, La, Sm, Eu, Yb and Lu; ± 5% for MgO, CaO, K_2O, V, Tb, Dy, Hf and Ta; ± 5 - 10% for Ba, Ce, Nd, Ho, Th, Sr, Ga, Zn and Ni; 10 - 20% for U, Au and Ir respectively. The analyses of controls 73121, 75081 and BCR-1 agree very well with the several replicate analyses reported by others (Laul and Schmitt, 1973, 1974; Korotev et al., 1976; Baedecker et al., 1974; Wänke et al., 1974, Proc. Lunar Conf. 1973-1978).

The major- and trace-element abundances of the >90 μm and 20-90 μm fractions are identical (Tables 3-6), and we have averaged these two coarse fractions for comparison to the <20 μm fine fraction whose chemistry is quite different.

Major Element Characteristics

Among the major elements, FeO and particularly TiO_2 are strong indicators of mare material, whereas Al_2O_3 is a strong indicator of highland material. Thus, we have plotted TiO_2 and Al_2O_3 for bulk, coarse and fine fractions as a function of depth in Figures 6 and 7. For consistency, we have plotted calculated bulk values in all figures. For Figures 6 and 7, we make the following observations.

As TiO_2 content decreases from the top of section 70009 to the bottom of 70006, the Al_2O_3 content correspondingly increases, suggesting that decrease in the mare content is coupled with an increase in the highland component. However, the <20 μm fine fraction is consistently more feldspathic in composition at all depths; i.e., it is high in Al_2O_3, CaO, K_2O, Na_2O, light REE, and low in TiO_2, FeO, MnO, Cr_2O_3, Sc and

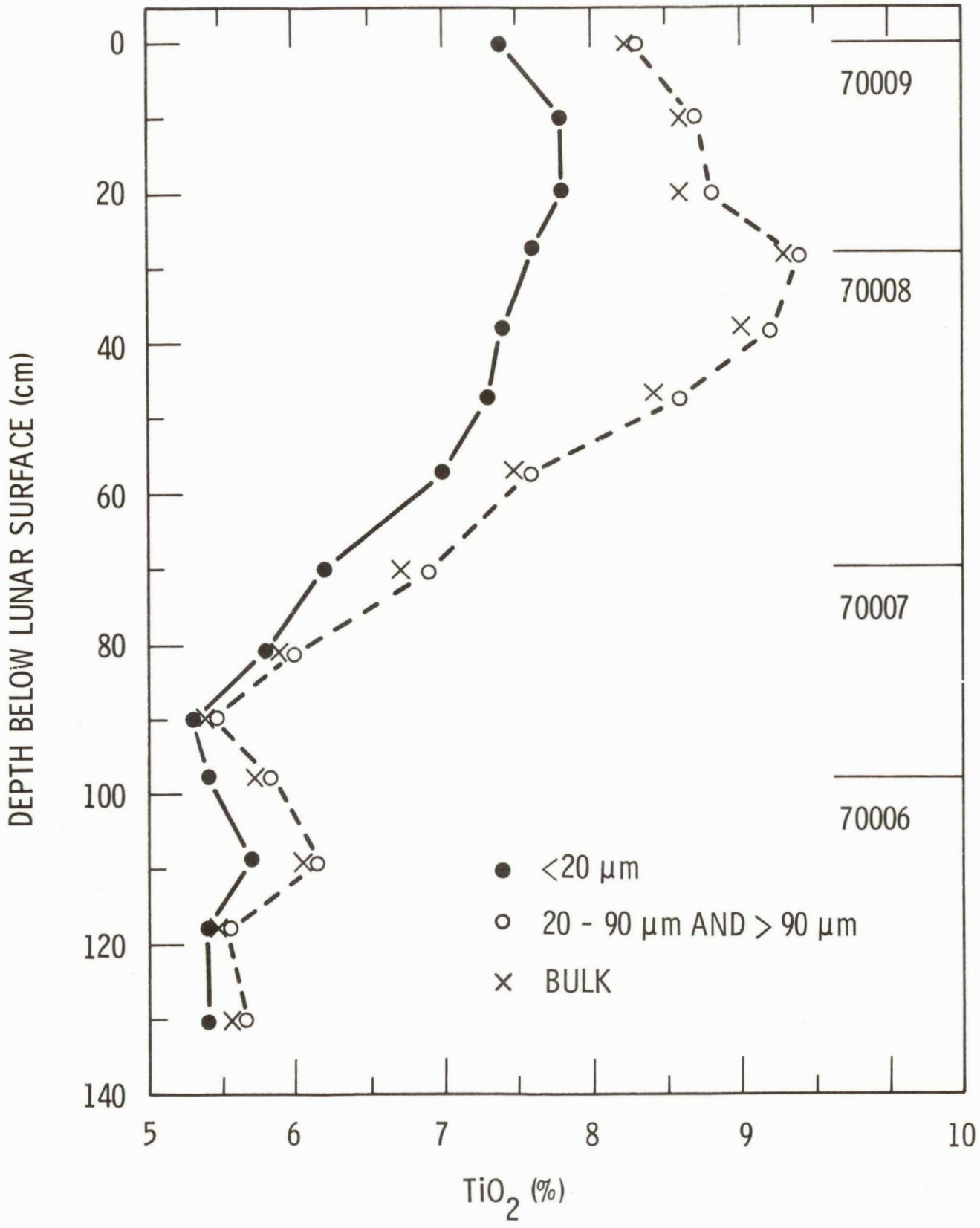

Figure 6. Depth profiles of TiO_2 in bulk, coarse (>90 µm and 20-90 µm) and <20 µm fine fractions of 70009-70006.

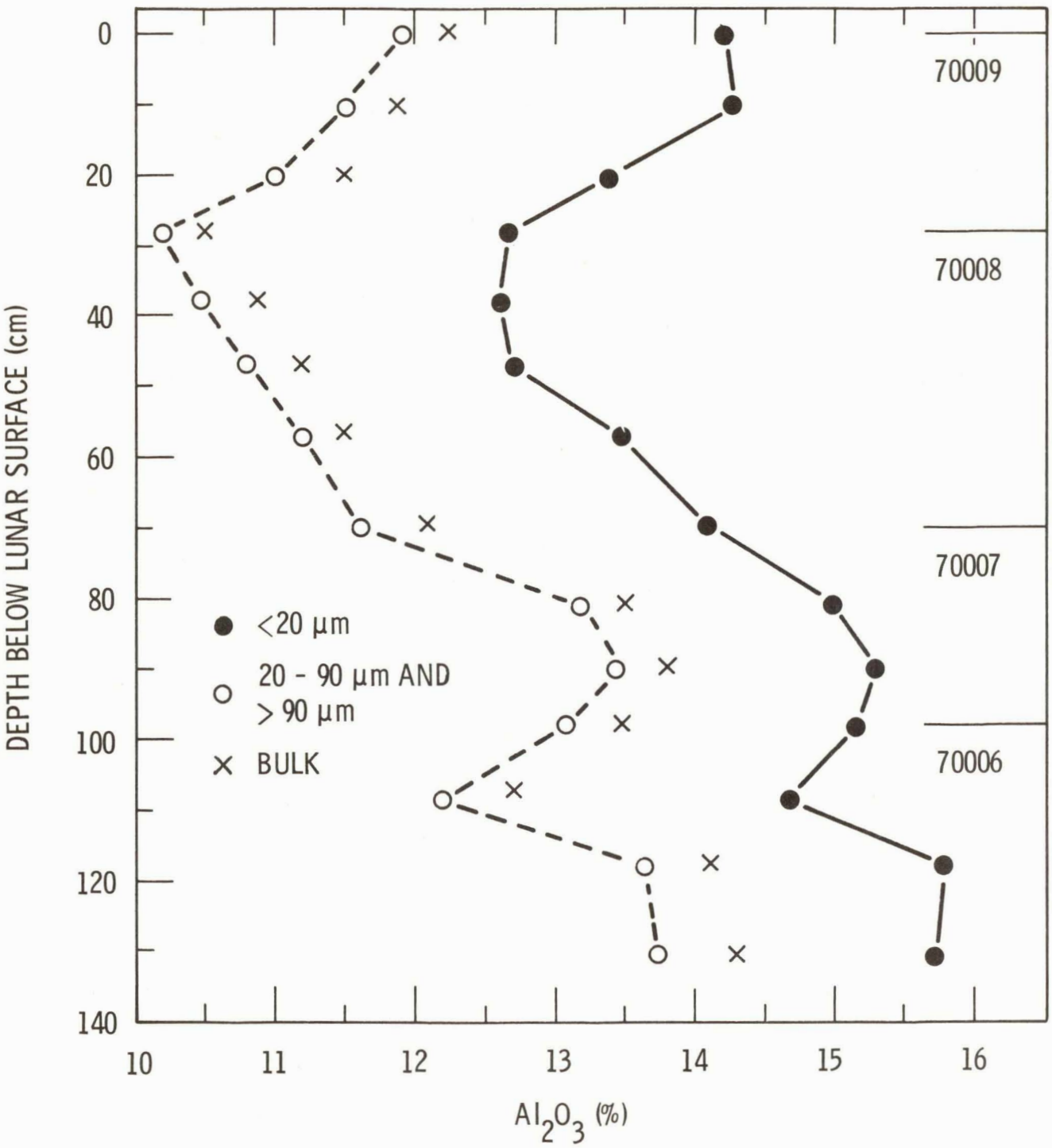

Figure 7. Depth profiles of Al_2O_3 in bulk, coarse (>90 µm and 20-90 µm) and <20 µm fine fractions of 70009-70006.

heavy REE relative to the >90 μm and 20-90 μm fractions. The fine (< 20 μm) fraction is considerably enriched in highland material, consistent with the observations of Korotev (1976). The bulk soil chemistry is governed by the coarse fractions because of their greater weight. The highland contribution in the <20 μm fraction generally increases from 45 to 81 cm depth, and below this depth the highland contribution stays about constant. The TiO_2 content in the <20 μm and coarse fractions tends to merge at ∿4.5-5.5% TiO_2 below 90 cm depth, suggesting that the coarse and bulk fractions like the fine fractions are dominated by highland instead of mare material. This is also supported by the large-ion lithophile (K, REE and Th) trace-element data discussed below.

The X-ray Unit 59, which includes core 70008, is a coarse-grained interval which extends from 25 to 80 cm depth (Duke and Nagle, 1974). We analyzed 5 samples at ∿10 cm depth intervals in 70008. The TiO_2 contents in samples at 28, 38 and 47 cm depth intervals are quite high (8.3-9.4%), in the range of typical high Ti mare basalt. Vaniman and Papike (1977a) and Taylor et al. (1977) found that this unit consists almost entirely of mare material (basalt + orange glass). Our TiO_2 modal data (table 2) and LIL patterns (discussed later) are consistent with this interpretation.

Figure 8 shows the depth profile of FeO and Sc in bulk soils and in size fractions. In the coarse fractions (>90 μm and 20-90 μm). FeO and Sc tend to follow TiO_2 content as indicators of the ilmenite basalt component. When the TiO_2 content is high (7-9%) the FeO (18-19%), and Sc (60-70 ppm) are also high, suggesting that much of the Sc is in the minerals of the ilmenite basalt. The distribution coefficients (D)

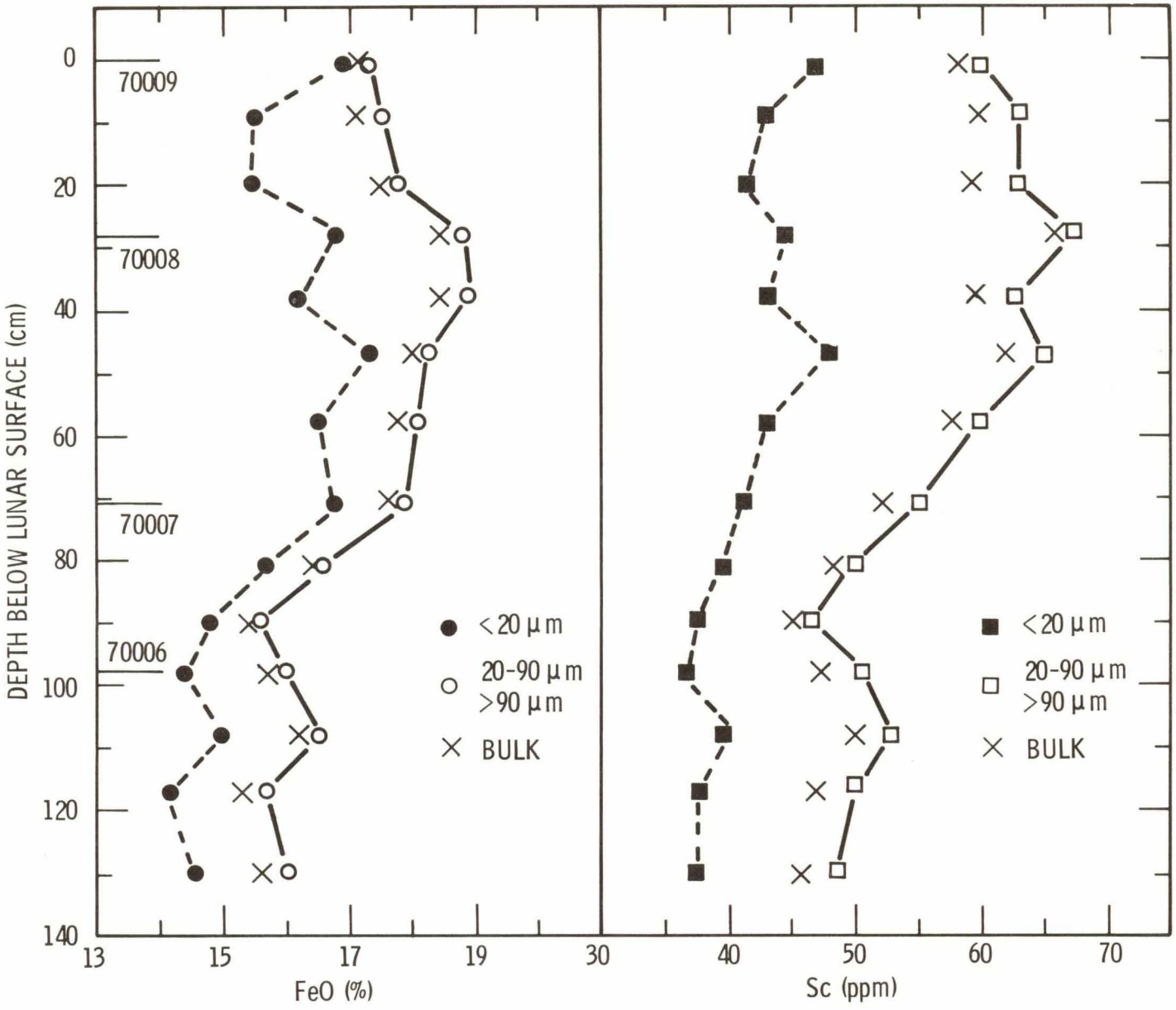

Figure 8. Depth profiles of FeO and Sc in bulk, coarse (> 90 µm and 20-90 µm) and < 20 µm fine fractions of 70009-70006. When TiO_2 is high (7-9%, see Fig. 6), FeO and Sc are high; when TiO_2 is low (∿ 5%), FeO and Sc are low, suggesting high Sc is related partly to the high ilmenite content.

of Sc in pyroxene and ilmenite of ilmenite basalt are 3.3 and 1.8 respectively (Haskin and Korotev 1977). Because of the higher proportion of ilmenite basalt in coarse soil fractions, the FeO/Sc ratios deviate significantly from the lunar FeO/Sc ratios or 5000 ± 500 (Laul and Schmitt, 1974; Wänke et al., 1974; Laul et al., 1978). When TiO_2 is low (5.5%) as in core segment 70006, FeO (∿16%) and Sc (∿50 ppm) are also low. In the cases of low TiO_2 content (1-2%), the FeO/Sc ratio follows the lunar ratio. In general, the coarse fractions contain considerable amounts of mare basalt and core section 70008 contains the highest mare contribution. The fine fractions contain consistently less mare basalt (less TiO_2, FeO, Sc, etc.) relative to the coarse fractions. This again emphasizes the dominance of highland material in the fine fractions.

The strong correlation between FeO and MnO with the FeO/MnO ratio of 80 ± 5 has been well established in a wide variety of lunar rocks and soils (Laul et al., 1972, 1974, 1978; Miller et al., 1974; Wänke et al., 1974). Mn^{++}(0.80 Å) can readily replace Fe^{++}(0.74 Å) in oxides and Mg-Fe silicates (pyroxene, olivine, etc.). Ehmann and Ali (1977), in their analyses of 26 bulk samples from 70009-70007 reported a range of 62-85 in the FeO/MnO ratios. This prompted them to suggest a third component with a much lower FeO/MnO ratio in order to account for their generally low FeO/MnO ratios. However, in the samples analyzed by us (Tables 3 and 4), tne FeO/MnO ratios are remarkably constant at 80 ± 5 in bulk soils and all size fractions. Thus, we find no evidence of fractionation between FeO and MnO.

The ratio CaO/Al_2O_3 reflects the relative proportion of plagioclase. In bulk soils and size fractions this ratio is constant above and below the coarse-grained layer (unit 2). The coarse layer (unit 2: 70008) has the higher CaO/Al_2O_3 suggesting a significant contribution

of mare material (pyroxene + ilmenite + orange glass), in both fine and coarse fractions. The coarse fractions at 28, 38 and 47 cm depths with CaO/Al_2O_3 ratios of 1.05 approach high-Ti mare basalt (CaO/Al_2O_3 = 1.1 to 1.2) and thus appear to be derived almost totally from mare basaltic material. Our qualitative interpretation is consistent with our LIL trace data and with the petrographic studies on the monomineralic component (0.02-2 mm) by Vaniman and Papike (1977b), which suggest 61% pyroxene and 26% plagioclase in the coarse section of 70008, and about 50% pyroxene and 30% plagioclase in sections 70009 and 70007. The Fe/Fe + Mg ratios, which reflect the pyroxene/olivine proportions, do not vary significantly both in the coarse and fine fractions of the entire core 70009-70006, indicating that the relative proportions of pyroxene and olivine are about constant. This is also supported from the modal data on coarse fractions (Table 2).

Large-ion Lithophile Patterns (K, REE and Th)

The chondritic normalized K, REE and Th (LIL) patterns in bulk soils and >90 μm, 20-90 μm and <20 μm size fractions are displayed in Figure 9. The LIL patterns of intermediate depths essentially follow the same general trend. Solid circles shown for some of the <20 μm fractions are representative analyses plotted to show the well defined patterns. In other samples, only lines are drawn in to avoid crowding. These patterns reveal the following observations:

1) The steep positive slopes of light REE or La/Sm ratios in the coarse fractions >90 μm and 20-90 μm are typical of mare material, whereas the enhanced La/Sm ratio in the fine fraction <20 μm indicates a significant contribution of highland material, consistent with the observation of Korotev (1976).
2) With increasing depth (except in coarse core 70008) the light REE slopes (La/Sm ratio) in the coarse fractions tend to flatten with

an increase in highland-type material. The <20 μm fractions also become more enriched in highland material with increasing depth.

3) The absolute concentration of La-Sm is in general higher in the fine than in the coarse fraction, though both fractions tend to merge at or below depths of 118 cm.

4) Both coarse and fine fractions exhibit a significant negative Eu anomaly. The absolute concentration of Eu is consistently higher in the fine fraction, although the Sm/Eu ratio of 1.65 is about the same in both coarse and fine fractions.

5) The K concentration in the fine fraction is consistently higher relative to the coarse fractions. In both fine and coarse fractions K increases with depth in the core but the relative differences between the two fractions do not change significantly.

6) In the coarse fractions, Th inflection is downward (characteristic of mare material) from the core top to 47 cm depth. Below this depth, it levels off (58 cm depth) and then shows an upward trend (characteristic of highland material). In the fine fractions, Th inflection is always upward (except for layers at 28 and 38 cm where it levels off).

The observations (1) and (2) confirm our earlier conclusion based on stratigraphy of TiO_2 and Al_2O_3 content; i.e., the fine fraction in each core segment is considerably enriched in highland material whose contribution, except in 70008 core, generally increases with depth. The coarse fractions at the top (70009) core are also rich in the mare material and become gradually enriched in highland material with depth. The coarse and fine fractions tend to merge towards the bottom core 70006 (figure 9).

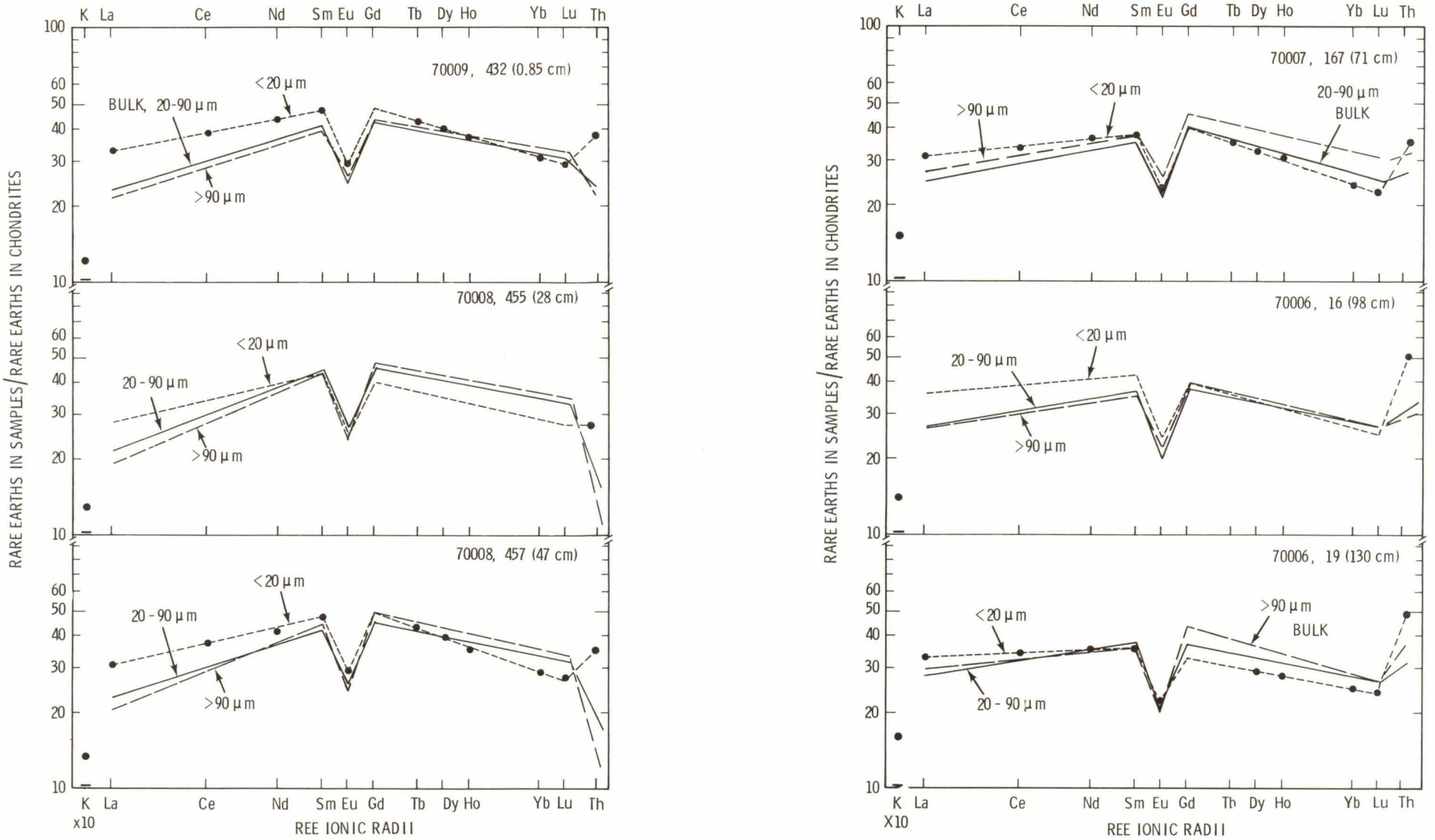

Figure 9. Chondritic normalized large-ion lithophile (K, REE and Th) patterns in bulk, > 90 µm, 20-90 µm and < 20 µm size fractions at six depth levels. Solid circles are the experimental points to show well-defined patterns. In other samples, only lines are drawn in to avoid crowding.

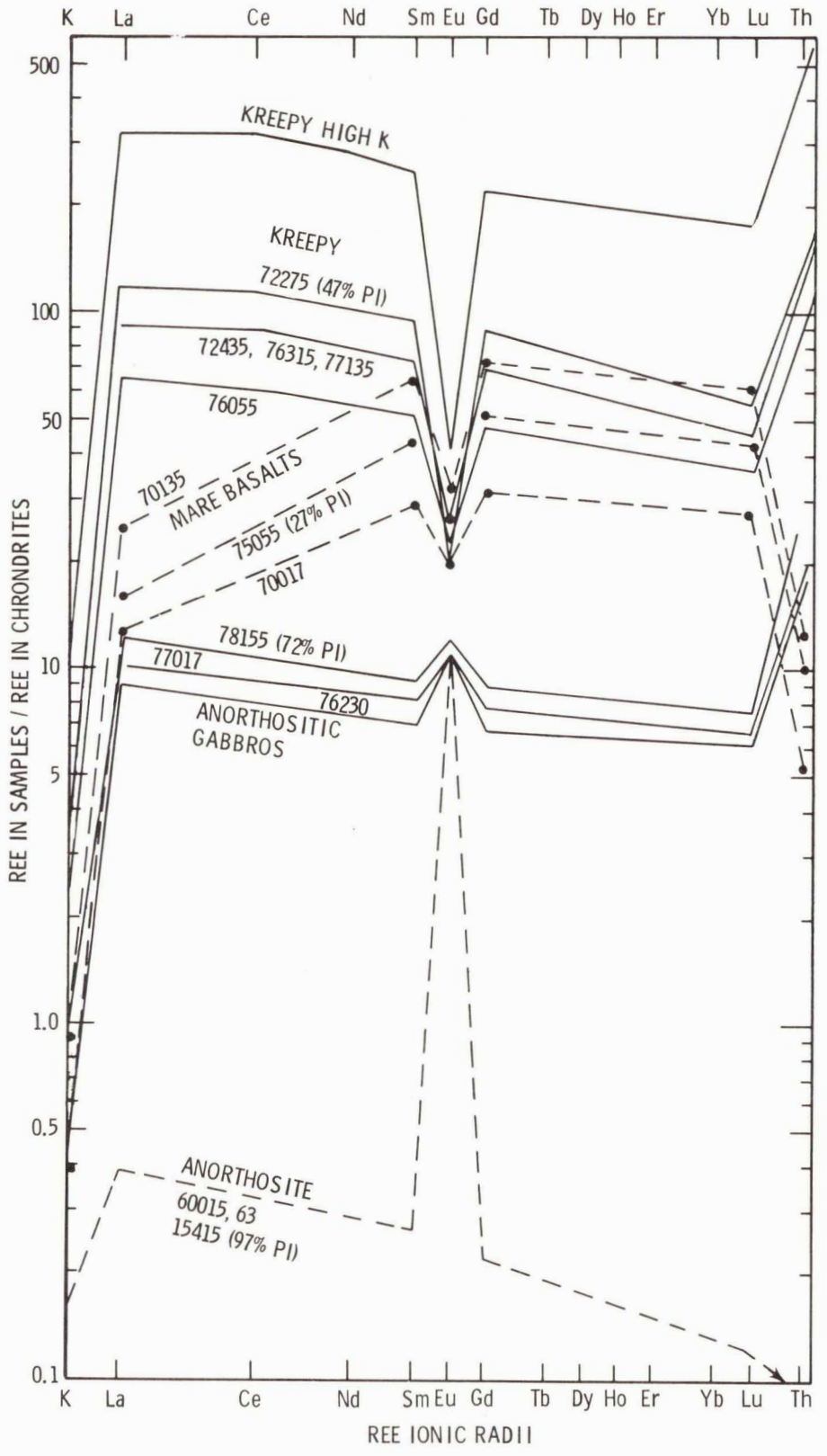

Figure 10. Chondritic normalized LIL (K, REE and Th) patterns and their ranges in anorthosites 60015,63 and 15415, anorthositic gabbros 76230, 77017 and 78155, mare basalts 70017, 75055 and 70135, med-K KREEP 76055, 72435, 76315, 77135 and 72275, and high-K KREEP. Sources for data are from LSPET (1973) and Proc. Lunar Sci. Conf. (1974-1978).

Is the highland component anorthositic (anorthosite-anorthositic gabbro) or KREEPy? Korotev (1976) used a 5-component (mare basalt, orange glass, KREEP, anorthositic gabbro and meteoritic) mixing model to show that both low-K KREEP and anorthositic gabbro are required as highland components to satisfy mass balance in the 90-150 μm and <20 μm fractions. As mentioned earlier, we plan to follow a similar multielement mixing model after complete study of the remaining core (70005-70001). However, using our present data on La, Sm, Eu and Th patterns we can characterize the dominant highland source and estimate the KREEP contribution in the <20 μm fractions (table 7). Our conclusions are consistent with Korotev (1976); e.g. our mean value of ∿16% low-K KREEP in the <20 μm fraction of 70008 core agrees well with the 16% low-K KREEP estimate obtained by Korotev (1976).

Figure 10 shows the LIL (K, REE and Th) patterns and their ranges in anorthosites 60015,63 and 15415 (97% plagioclase), anorthositic gabbros 76230, 77017 and 78155 (72% plagioclase), mare basalts 70017, 75055 and 70135, med-K KREEP 76055, 72435, 76315, 77135 and 72275, and high-K KREEP (LSPET, 1973; Lunar Proc. Volume 1974-1978).

These patterns show that relative Th abundance is a strong indicator of KREEP and can easily distinguish KREEPy from mare and anorthositic material. The La/Sm ratios (light REE) can distinguish mare from KREEPy and anorthositic materials. Thus REE concentrations and Sm/Eu ratios play an important role in distinguishing among these components. With these guidelines we can reexamine the LIL patterns (Figure 9) more closely, particularly in light of Th.

In the top of the core (70009,432), Th in the coarse fraction

is depleted relative to Lu (inflection downward) characteristic of mare material whereas the fine fraction has upward Th inflection characteristic of KREEPy material. The same trend exists in layers at 10 and 20 cm in 70009. In the 28 cm layer of the coarse unit (70008) Th in the coarse fractions is almost characteristic of mare material because of its steep downward inflection, but the fine fraction shows virtually no inflection of Th suggesting low contribution of KREEPy material. The same trends are found at 38 cm depth (70008,456). At 47 cm and 58 cm depths, Th in the fine fractions shows slight upward trends while it still has a downward inflection in the coarse fractions. At 70 cm depth (70007,167) Th in both the coarse and fine fractions shows an upward trends. These upward trends increase somewhat with depth and level off towards the base of section 70006. Such smooth transitional changes in Th inflections from the top to the bottom of the core suggest that the highland source in these cores (and especially in the fine fraction) is KREEPy instead of anorthositic. A pure anorthositic source can be ruled out because the absolute REE (except Eu) and Th concentrations are far too low to cause any observable change between coarse to fine fractions. If anorthositic gabbro were the sole source it would have to be present in great abundance ($\geq$50%) to affect the magnitude of chemical differences we observe between the coarse and fine fractions. However, this would also affect the Sm/Eu ratios in the fine relative to the coarse fraction contrary to our observation (4): the Sm/Eu ratio is about constant at 1.65 in both the coarse and fine fractions. Based on Eu constraints we estimate about 10% anorthositic gabbroic material in the fine relative to the coarse fraction. This is in reasonable agreement with the estimates of Korotev (1976).

Table 7. Low-K KREEP* contribution in <20 μm fine fractions of 70009-70006 cores

Sample	Depth (cm)	In excess of coarse fraction Based on Th (%)	In excess of coarse fraction Based on La (%)	Total value[a] Based on Th (%)
70009, 432	0.85	11	11	22
70009, 433	9.4	17	12	28
70009, 434	20.4	8.0	7.0	17
70008, 455	28.0	11	8.4	13
70008, 456	38.0	12	8.0	15
70008, 457	47.0	15	10	19
70008, 458	57.5	6.2	7.8	17
70007, 167	70.6	5.8	5.4	21
70007, 168	81.0	11	10	23
70007, 169	89.6	6.3	4.1	26
70006, 16	98.0	14	11	30
70006, 17	108	12	11	27
70006, 18	117	12	9.9	29
70006, 19	130	10	6.0	29

* Based on Th = 130X (chondrites); La = 90X

a. Mare indigenous value is taken as 10X.

The noritic breccias collected at the Apollo 17 site are mostly low-K KREEP (LSPET, 1973). The low-K KREEP is very similar to low-K Fra Mauro basalts abundant in the highlands (Apollo 14, 15 and 16, and Luna 20 sites). In order to estimate the KREEP contribution in the fine fraction, we use La and Th as indicators for KREEP. Since low-K KREEP shows a range in LIL abundances (Figure 10), we have simply taken the mean value of La (90X chondritic) and Th (130X) in KREEPy rocks to represent low-K KREEP. The mean Th in mare basalts is taken as 10X (Figure 10).

We have calculated KREEPy contribution in the fines in two ways: 1) by subtracting the coarse contribution (>90 μm and 20-90 μm) using La and Th as indicators; and 2) by subtracting the mare basalt contribution (Th = 10X chondritic). The latter method yields the total KREEP contribution in the fine fraction, since Th in mare material (basalt + orange glass) is relatively small. The results are tabulated in Table 7. The total low-K KREEP varies from 13-30% in the fine fraction. It is low in the coarse unit core 70008, and increases below 57 cm depth and levels off to 29% at the base of the 70006. The average total KREEP contribution is ∿22% in the fine soil fraction. Moreover, the fine fractions contain on the average ∿11% (6-17%) more low-K KREEPy material than the coarse soils.

Transport of Fine Fraction

The highland enrichment in the fine fraction raises other questions. Is the transport of fine fraction a local phenomenon or does it extend from distant localities? Is transport mainly lateral or vertical? Korotev (1976) in his meticulous grain size study of Apollo 17 soils suggested the north and south massifs as the local source for "KREEPy" components added to the valley floor soil as

fine-grained material. The soils and boulders from the massifs are feldspathic in composition, and their LIL abundances lie in the range of medium-K and low-K KREEP respectively (LSPET, 1973, Lunar Proc. 1973-1975). The argument for a source area in the massifs is supported by the fact that the KREEP contribution in the coarse (90-150 μm) and fine (<20 μm) fractions from the south massif soil 72150 (Korotev, 1976) show the expected pattern of low-K KREEP enrichment relative to the valley soils.

Korotev (1976) reported a similar highland enrichment in the <20 μm fraction from Apollo 11 soil 10084. Boynton and Wasson (1977) noticed a similar effect in their 20-7 μm and < 7 μm fractions of Apollo 15 soil 15100. Their work, coupled with our systematic study of Apollo 17 soils, tends to suggest that the fine fraction from mare soils is in general enriched in highlands (KREEPy) material.

In the case of the Apollo 17 site, the massifs are at higher elevation than the mare valley and have been constantly bombarded by meteorites and micrometeorites with the result that highland material tends to be finer than mare materials on the valley floor. At the Apollo 17 site the elevated massifs provide favorable sites for lateral and downward mixing of highland materials into the dominating mare regolith in the valley of Taurus Littrow. However, the lack of large-scale geochemical gradients at highland/mare contacts argues against efficient lateral transport of highland material across mare areas (Horz, 1978; Hubbard and Villas, 1977). Cratering calculations of Arvidson et al. (1975), and Quaide and Oberbeck (1975) also argue against any significant lateral transport over distances >>10 Km. It is perhaps possible that the scaling laws do not extend to fine

fractions. Nevertheless, our arguments for lateral transport of a few Km (∿10 Km) is consistent within the constraints of cratering and orbital X-ray calculations.

Depth Profile of Zn

Figure 11 shows the depth profile of Zn in <20 μm fine fractions of 70009-70006. For typical size distribution, we have included two histograms; one at the surface and the other at 108 cm depth. Zn is unusually high and its depth profile is quite variable. We have ruled out the possibility of Zn contamination because the calculated mass balance agrees well with bulk soil analyses (Tables 5 and 6). We attribute such high Zn abundances to indigenous mare volatile concentrations (Zn, Cd, Se, etc.).

The source for volatiles appears to be high-Ti mare glasses. The drill core contains a significant amount of high-Ti orange and black glasses (∿10-15% of the > 20 μm fraction; Vaniman and Papike, 1977b; Taylor et al., 1977). Morgan et al. (1975) reported 140 ppm of Zn in orange glass and 45 ppm of Zn in dark glass. About 30% contribution of orange glass will yield 42 ppm Zn, which matches our Zn values in bulk soils. The orange glasses are considered to have been formed as a result of volcanic vent activity (Meyer et al., 1975; Heiken and McKay, 1977). The released volatiles seem to reside on the surface of glass droplets and thus are surface correlated (Boynton and Wasson, 1977; Krähenbühl et al., 1976). Because of the large surface concentration and small grain size, Zn enrichment would be greatly increased in the fine fraction, consistent with our data. The Zn in the > 90 μm and 20-90 μm fractions are about the same, suggesting

CONCLUSIONS

This paper is essentially a progress report and presentation of data. Our final conclusions must await completion of our study, including core sections 70005 through 70001. Preliminary conclusions are listed below.

1. The chemistry of the > 90 μm and 20-90 μm coarse fractions is identical but quite different from the < 20 μm fine fraction.
2. The upper 50 cm of the drill core is highly enriched in mare material (basalt + orange glass). The coarse fractions at 28, 38 and 47 cm depth appear to consist almost totally of mare material. Below the 58 cm depth all size fractions show a gradual decrease of mare material and an increase of highland material. At ∿ 90 cm depth these changes level out.
3. The dominant source of highland material is KREEPy instead of anorthositic. Relative to the coarse fractions, the fine fraction contains about 10% more of this low-K KREEPy material. This KREEPy excess can be best explained by lateral (∿ 10 km) movement of fines from local massifs (consistent with the conclusion of Korotev, 1976).
4. Highland enrichment in the fine fractions of Apollo 17 soils, coupled with similar observations in Apollo 11 soil 10084 (Korotev, 1976) and Apollo 15 soil 15100 (Boynton and Wasson, 1977), suggests that this enrichment may perhaps be moonwide. However, the contributing sources are likely to be local at each site.

5. Indigenous volatiles such as Zn are quite high in all size fractions, but the most notable depth variation is seen in the < 20 μm fraction. A pronounced Zn peak in the fine fraction of the coarse layer (∿ 30-70 cm depth) might be correlated with an abundance of < 20 μ orange glass.

ACKNOWLEDGEMENTS

J. C. Laul is highly indebted to W. C. Richey of Battelle Northwest Laboratory for his assistance in the INAA experiments. He thanks R. A. Schmitt and M.-S. Ma of Oregon State University for the use of their counting equipment for short irradiations. We benefitted from the critical reviews of L. A. Haskin and G. J. Taylor. The assistance of the reactor crew at the OSU TRIGA reactor is appreciated. Si was measured using Dow Chemical's facility at Midland, Michigan, and the assistance of M. Kocsis in Si determinations is appreciated. This work was supported by NASA Grants NGL-33-015-130 and NSG-9044 which we gratefully acknowledge. We wish to extend our special thanks to D. McKay and G. Waits for their help in sieving the soil samples.

REFERENCES

Arvidson R., Drozd R.J., Hohenberg C.M., Morgan C.J. and Poupeau G. (1975) Horizontal transport of the regolith, modification of features, and erosion rates on the lunar surface. The Moon 13, 67-79.

Baedecker P. A., Chou C. L., Sundberg L. L. and Wasson J. T. (1974) Volatile and siderophilic trace elements in the soils and rocks of Taurus-Littrow. Proc. Lunar Sci. Conf. 5th, 1625-1643.

Bence A. E. and Albee A. L. (1968) Empirical correction factors for electron microanalysis of silicates and oxides. J. Geol. 76, 382-403.

Bence A. E., Delano J. W., Papike J. J. and Cameron K. L. (1974) Petrology of the highlands massifs at Taurs-Littrow: An analysis of the 2-4 mm soil fraction. Proc. Lunar Sci. Conf. 5th, 785-827.

Boynton W. V. and Wasson J. T. (1977) Distribution of 28 elements in size fractions of lunar mare and highlands soils. Geochim. Cosmochim. Acta 41, 1073-1082.

Crozaz G. and Plachy A. L. (1976) Origin of the Apollo 17 deep drill coarse-grained layer. Proc. Lunar Sci. Conf. 7th, 123-131.

Curtis D. and Wasserburg G. J. (1975) Apollo 17 neutron stratigraphy sedimentation and mixing in the lunar regolith. The Moon 13, 185-227.

Duke M. B. and Nagle J. S. (1974) Lunar Core Catalog, NASA Publication JSC 09252, 1-242.

Ehmann W. D. and Ali M. Z. (1977) Chemical stratigraphy of the Apollo 17 deep drill cores 70009-70007. Proc. Lunar Sci. Conf. 8th, 3223-3241.

Flanagan F. J. (1973). 1972 values for international geochemical reference sample. Geochim. Cosmochim. Acta 37, 1189-1200.

Haskin L. A. and Korotev R. L. (1977) Test of a model for trace element partition during closed-system solidification of a silicate liquid. Geochim. Cosmochimica Acta 41, 921-939.

Heiken G. and McKay D. S. (1977). A model for eruption behavior of a volcanic vent in eastern Mare Serenitatis. Proc. Lunar Sci. Conf. 8th, 3243-3255.

Hörz F. (1978) How thick are lunar mare basalts? (abstract). In Lunar and Planetary Science IX, 540-542. Lunar and Planetary Institute.

Hubbard N. J. and Vilas F. (1977) From Serenity to Langemak: A regional chemical setting for Crisium. In Papers Presented to the Conference on Luna 24, 85-88. The Lunar Science Institute, Houston.

Korotev, R. L. (1976) Geochemistry of grain-size fraction of soils from the Taurus-Littrow Valley floor. Proc. Lunar Sci. Conf. 7th, 695-726.

Krähenbühl U., Grütter A., Von Gunten H. R., Meyer G., Wegmuller F. and Wyttenbach A. (1977) Volatile and non-volatile elements in grain-size fraction of Apollo 17 soils 75081, 72461, and 72501. Proc. Lunar Sci. Conf. 8th, 3901-3916.

Laul J. C., Hill D. W. and Schmitt R. A. (1974) Chemical studies of Apollo 16 and 17 samples. Proc. Lunar Sci. Conf. 5th, 1047-1066.

Laul J. C. and Rancitelli L. A. (1977) Multielement analysis by sequential instrumental and radiochemical neutron activiation. J. Radioanal. Chem. 38, 461-475.

Laul J. C. and Schmitt R. A. (1973) Chemical composition of Apollo 15, 16 and 17 samples. Proc. Lunar Sci. Conf. 4th, 1349-1367.

Laul J. C., Vaniman D. T. and Papike J. J. (1978) Chemistry, mineralogy and petrology of seven > 1 mm fragments from Mare Crisium. In Mare Crisium: The View from Luna 24 (R. B. Merrill and J. J. Papike, Eds.), in press.

Laul J. C., Wakita H., Schowalter D. L., Boynton W. V. and Schmitt R. A. (1972) Bulk, rare earth and other trace elements in Apollo 14 and 15 and Luna 16 samples. Proc. Lunar Sci. Conf. 3rd, 1181-1200.

LSPET (1973) Apollo 17 preliminary science report. JSC SP-330, 1-37.

McKay D. S., Fruland R. M. and Heiken G. H. (1974) Grain size and evolution of lunar soils. Proc. Lunar Sci. Conf. 5th, 887-906.

McCallum J. S., Mathez E. A., Okamura F. P. and Gose S. (1974) Petrology and crystal chemistry of Poikilitic anorthositic gabbro 77017. Proc. Lunar Sci. Conf. 5th, 287-302.

Meyer C. Jr., McKay D. S., Anderson D. H. and Butler P. Jr. (1975). The source of sublimates on the Apollo 15 green and Apollo 17 orange glass samples. Proc. Lunar Sci. Conf. 6th, 1673-1699.

Miller M. D., Pacer R. A., Ma M.-S., Hawke B. R., Lookhart G. L. and Ehmann W. D. (1974) Compositional studies of the lunar regolith at the Apollo 17 site. Proc. Lunar Sci. Conf. 5th, 1079-1086.

Morgan J. W., Ganapathy R., Higuchi H., Krähenbühl U. and Anders E. (1974) Lunar basins: tentative characterization of projectiles from meteoritic elements in Apollo 17 boulders. Proc. Lunar Sci. Conf. 5th, 1703-1736.

Morris R. V., Gose W. A. and Lauer H. V. Jr. (1978) Maturity and FeO profiles for the Apollo 17 deep drill core. Lunar Sci. IX, 766-768.

Papike J. J., Vaniman D. T., Schweitzer E. L. and Baldwin K. (1978) Apollo 16 drive tube 60009/60010, Part III. Total major element partitioning among the regolith components or chemical mixing models with petrologic credibility. Lunar Sci. IX, 862-864.

Proc. Lunar Sci. Conf. 2nd to 8th (1970-1977), Vols. 1, 2, 3.

Quide W. L. and Oberbeck V. R. (1975). The Moon 5, 27-55.

Takahashi H., Janssens M. J., Morgan J. W. and Anders E. (1978) Further studies of trace elements in C_3 chondrites. Geochim. Cosmochim. Acta 42, in press.

Taylor G. J., Wentworth S., Warner R. D. and Keil K. (1978) Petrology of Apollo 17 deep drill core - II: Agglutinates as recorders of fossil soil compositions (abstract) Lunar and Planetary Science IX, 1146-11148. Lunar and Planetary Institute, Houston.

Taylor G. J., Keil K. K. and Warner R. D. (1977a) Petrology of Apollo 17 deep drill core: Depositional history based on modal analyses of 70009, 70008, and 70007. Proc. Lunar Sci. Conf. 8th, 3195-3222.

Taylor G. J., Keil K. and Warner R. D. (1977b) Very low-Ti mare basalts. Geophys. Res. Lett. 4, 207-210.

Vaniman D. T. and Papike J. J. (1977a) The Apollo 17 drill core: Characterization of the mineral and lithic component (Sections 70007, 70008, 70009). Proc. Lunar Sci. Conf. 8th, 3123-3159.

Vaniman D. T. and Papike J. J. (1977b) The Apollo 17 drill core: Modal petrology and glass chemistry (Section 70007, 70008, 70009). Proc. Lunar Sci. Conf. 8th, 3161-3193.

Vaniman D. T. and Papike J. J. (1977c) Very low Ti (VLT) basalts: A new mare rock type from the Apollo 17 drill core. Proc. Lunar Sci. Conf. 8th, 1443-1471.

Vaniman D. T., Papike J. J. and Schweitzer E. (1978) Apollo 16 drive tube 60009/60010. Part II: Petrology and major element partitioning among the regolith components. Proc. Lunar and Planetary Sci. Conf. 9th (in press).

Wänke H., Palme H., Baddenhausen H., Dreibus G., Jagoutz E., Kruse H., Spettel B., Teschke F., and Thacker R. (1974) Chemistry of Apollo 16 and 17 samples: Bulk composition late-stage accumulation and early differentiation of the moon. Proc. Lunar Sci. Conf. 5th, 1307-1355.